Glatt H, Schneider H, Liu Y. 2005. V79-hCYP2E1-hSULT1A1, a cell line for the sensitive detection of genotoxic effects induced by carbohydrate pyrolysis products and other food-borne chemicals. Mutat Res 580:41–52.

Hakura A, Shimada H, Nakajima M, Sui H, Kitamoto S, Suzuki S, Satoh T. 2005. Salmonella/human S9 mutagenicity test: A collaborative study with 58 compounds. Mutagen 20:217–228.

Hargreaves MB, Jones BC, Smith DA, Gescher A. 1994. Inhibition of *p*-nitrophenol hydroxylase in rat liver microsomes by small aromatic and heterocyclic molecules. Drug Metab Dispos 22: 806–810.

Hashimoto K, Tanii H. 1985. Mutagenicity of acrylamide and its analogues in *Salmonella typhimurium*. Mutat Res 158:129–133.

Honma M, Hayashi M, Sofuni T. 1997. Cytotoxic and mutagenic responses to X-rays and chemical mutagens in normal and p53-mutated human lymphoblastoid cells. Mutat Res 374:89–98.

IARC. Acrylamide. In:IARC Monographs on the Evaluation of Carcinogen Risk to Human: Some Industrial Chemicals, Vol. 60. Lyon: International Agency for Research on Cancer. Lyon. 1994. pp 389–433.

Ikeda T, Nishimura K, Taniguchi T. 2001. In vitro evaliation of drug interaction caused by enzyme inhibition-HAB protocol. Xenobiol Metabol Dispos 16:115–126.

Knaap AG, Kramers PG, Voogd CE, Bergkamp WG, Groot MG, Langebroek PG, Mout HC, van der Stel JJ, Verharen HW. 1988. Mutagenic activity of acrylamide in eukaryotic systems but not in bacteria. Mutagen 3:263–268.

Koyama N, Sakamoto H, Sakuraba M, Koizumi T, Takashima Y, Hayashi M, Matsufuji H, Yamagata K, Masuda S, Kinae N, Honma M. 2006. Genotoxicity of acrylamide and glycidamide in human lymphoblastoid TK6 cells. Mutat Res 603:151–158.

Lahdetie J, Suutari A, Sjoblom T. 1994. The spermatid micronucleus test with the dissection technique detects the germ cell mutagenicity of acrylamide in rat meiotic cells. Mutat Res 309:255–262.

Manjanatha MG, Aidoo A, Shelton SD, Bishop ME, MacDaniel LP, Doerge DR. 2005. Evaluation of mutagenicity in Big Blue (BB) mice administred acrylamide (AA) and glycidamide (GA) in drinking water for 4 weeks. Environ Mol Mutagen 44:214.

Matsushima T, Hayashi M, Matsuoka A, Ishidate M Jr, Miura KF, Shimizu H, Suzuki Y, Morimoto K, Ogura H, Mure K, Koshi K, Sofuni T. 1999. Validation study of the in vitro micronucleus test in a Chinese hamster lung cell line (CHL/IU). Mutagen 14:569–580.

Mei N, Hu J, Churchwell MI, Guo L, Moore MM, Doerge DR, Chen T. 2008. Genotoxic effects of acrylamide and glycidamide in mouse lymphoma cells. Food Chem. Toxicol 46:628–636.

Moore MM, Amtower A, Doerr C, Brock KH, Dearfield KL. 1987. Mutagenicity and clastogenicity of acrylamide in L5178Y mouse lymphoma cells. Environ Mutagen 9:261–267.

Mottram DS, Wedzicha BL, Dodson AT. 2002. Acrylamide is formed in the Maillard reaction. Nature 419:448–449.

Oda Y, Nakamura S, Oki I, Kato T, Shinagawa H. 1985. Evaluation of the new system (umu-test) for the detection of environmental mutagens and carcinogens. Mutat Res 147:219–229.

Oda Y, Aryal P, Terashita T, Gillam EM, Guengerich FP, Shimada T. 2001. Metabolic activation of heterocyclic amines and other procarcinogens in *Salmonella typhimurium* umu tester strains expressing human cytochrome P4501A1, 1A2, 1B1, 2C9, 2D6, 2E1, and 3A4 and human NADPH-P450 reductase and bacterial *O*-acetyltransferase. Mutat Res 492:81–90.

Omori T, Honma M, Hayashi M, Honda Y, Yoshimura I. 2002. A new statistical method for evaluation of L5178Ytk(+/−) mammalian cell mutation data using microwell method. Mutat Res 517:199–208.

Rice JM. 2005. The carcinogenicity of acrylamide. Mutat Res 580:3–20.

Sandhu P, Guo Z, Baba T, Martin MV, Tukey RH, Guengerich FP. 1994. Expression of modified human cytochrome P450 1A2 in *Escherichia coli*: Stabilization, purification, spectral characterization, and catalytic activities of the enzyme. Arch Biochem Biophys 309:168–177.

Segerback D, Calleman CJ, Schroeder JL, Costa LG, Faustman EM. 1995. Formation of *N*-7-(2-carbamoyl-2-hydroxyethyl)guanine in DNA of the mouse and the rat following intraperitoneal administration of [14C]acrylamide. Carcinogenesis 16:1161–1165.

Shelby MD, Cain KT, Cornett CV, Generoso WM. 1987. Acrylamide: Induction of heritable translocation in male mice. Environ Mutagen 9:363–368.

Sofuni T, Hayashi M, Matsuoka A, Sawada M. 1985. Mutagenicity tests on organic chemical concominants in city water and related compounds. II. Chromosome aberration tests in cultured mammalian cells. Eisei Shiken Hok 103:64–75.

Stadler RH, Blank I, Varga N, Robert F, Hau J, Guy PA, Robert MC, Riediker S. 2002. Acrylamide from Maillard reaction products. Nature 419:449–450.

Sumner SC, Fennell TR, Moore TA, Chanas B, Gonzalez F, Ghanayem BI. 1999. Role of cytochrome P450 2E1 in the metabolism of acrylamide and acrylonitrile in mice. Chem Res Toxicol 12:1110–1116.

Sumner SC, Williams CC, Snyder RW, Krol WL, Asgharian B, Fennell TR. 2003. Acrylamide: A comparison of metabolism and hemoglobin adducts in rodents following dermal, intraperitoneal, oral, or inhalation exposure. Toxicol Sci 75:260–270.

Suzuki S, Kurata N, Nishimura Y, Yasuhara H, Satoh T. 2000. Effects of imidazole antimycotics on the liver microsomal cytochrome P450 isoforms in rats: Comparison of in vitro and ex vivo studies. Eur J Drug Metab Pharmacokinet 25:121–126.

Tareke E, Rydberg P, Karlsson P, Eriksson S, Tornqvist M. 2000. Acrylamide: A cooking carcinogen? Chem Res Toxicol 13:517–522.

Tareke E, Rydberg P, Karlsson P, Eriksson S, Tornqvist M. 2002. Analysis of acrylamide, a carcinogen formed in heated foodstuffs. J Agric Food Chem 50:4998–5006.

Tornqvist M. 2005. Acrylamide in food: The discovery and its implications: A historical perspective. Adv Exp Med Biol 561:1–19.

Tsuda H, Shimizu CS, Taketomi MK, Hasegawa MM, Hamada A, Kawata KM, Inui N. 1993. Acrylamide; induction of DNA damage, chromosomal aberrations and cell transformation without gene mutations. Mutagen 8:23–29.

Wu YQ, Yu AR, Tang XY, Zhang J, Cui T. 1993. Determination of acrylamide metabolite, mercapturic acid by high performance liquid chromatography. Biomed Environ Sci 6:273–280.

Xiao Y, Tates AD. 1994. Increased frequencies of micronuclei in early spermatids of rats following exposure of young primary spermatocytes to acrylamide. Mutat Res 309:245–253.

Zeiger E, Anderson B, Haworth S, Lawlor T, Mortelmans K, Speck W. 1987. Salmonella mutagenicity tests. III. Results from the testing of 255 chemicals. Environ Mutagen 9(Suppl 9):1–109.

Accepted by—
K. Dearfield

Bioorganic & Medicinal Chemistry Letters 20 (2010) 260–265

Contents lists available at ScienceDirect

Bioorganic & Medicinal Chemistry Letters

journal homepage: www.elsevier.com/locate/bmcl

DNA methylation by dimethyl sulfoxide and methionine sulfoxide triggered by hydroxyl radical and implications for epigenetic modifications

Kazuaki Kawai, Yun-Shan Li, Ming-Fen Song, Hiroshi Kasai *

Department of Environmental Oncology, Institute of Industrial Ecological Sciences, University of Occupational and Environmental Health, 1-1, Iseigaoka, Yahatanishi-ku, Kitakyushu 807-8555, Japan

ARTICLE INFO

Article history:
Received 26 September 2009
Revised 23 October 2009
Accepted 27 October 2009
Available online 30 October 2009

Keywords:
5-Methyldeoxycytidine
Methyl radicals
Dimethylsulfoxide
Methionine sulfoxide
Epigenetic

ABSTRACT

In this Letter, we demonstrate the formation of m^5dC from dC or in DNA by dimethylsulfoxide (DMSO) and methionine sulfoxide (MetO), under physiological conditions in the presence of the Fenton reagent in vitro. DMSO reportedly affects the cellular epigenetic profile, and enhances the metastatic potential of cultured epithelial cells. The methionine sulfoxide reductase (Msr) gene was suggested to be a metastatis suppressor gene, and the accumulation of MetO in proteins may induce metastatic cancer. Our findings are compatible with these biological data and support the hypothesis that chemical cytosine methylation via methyl radicals is one of the mechanisms of DNA hypermethylation during carcinogenesis. In addition to m^5dC, the formation of 8-methyldeoxyguanosine (m^8dG) was also detected in DNA under the same reaction conditions. The m^8dG level in human DNA may be a useful indicator of DNA methylation by radical mechanisms.

Alkyl radicals, including methyl radicals, are generated from the tumor promoters, cumene hydroperoxide and *t*-butyl hydroperoxide in mouse keratinocytes, based on ESR experiments, suggesting that carbon radicals are involved in cancer induction.[1] In addition to these chemicals, the generation of methyl radicals from various carcinogens has been observed in vitro and in vivo. The metabolism of 1,2-dimethylhydrazine[2] and procarbazine[3] produces methyl radicals. Acetaldehyde generates methyl radicals by treatments with xanthine oxidase,[4] peroxynitrite,[5] and Fe^{2+}/H_2O_2.[5] The formation of a methyl radical - deoxyguanosine adduct, 8-methyl-2′-deoxyguanosine (m^8dG), has been detected in DNA after a treatment with *t*-butyl hydroperoxide and ferrous ion in vitro,[6] and after the administration of 1,2-dimethylhydrazine to rats.[7] Methylation of RNA purine bases at the C-8 position by methyl radicals has been also observed.[8] We recently reported that cytosine C-5 methylation in the monomer dC and DNA occurred via methyl radicals generated by the tumor promoters, cumene hydroperoxide and *t*-butyl hydroperoxide, in the presence of ferrous ion.[9] This discovery suggested new mechanisms of aberrant DNA hypermethylation in the epigenetic process during chemical carcinogenesis. Enzymatic DNA methylation due to the increased expression of DNA methyltransferases (DNMTs) is a widely accepted mechanism of DNA hypermethylation.[10,11] However, controversial data showing no clear association between gene hypermethylation in cancer

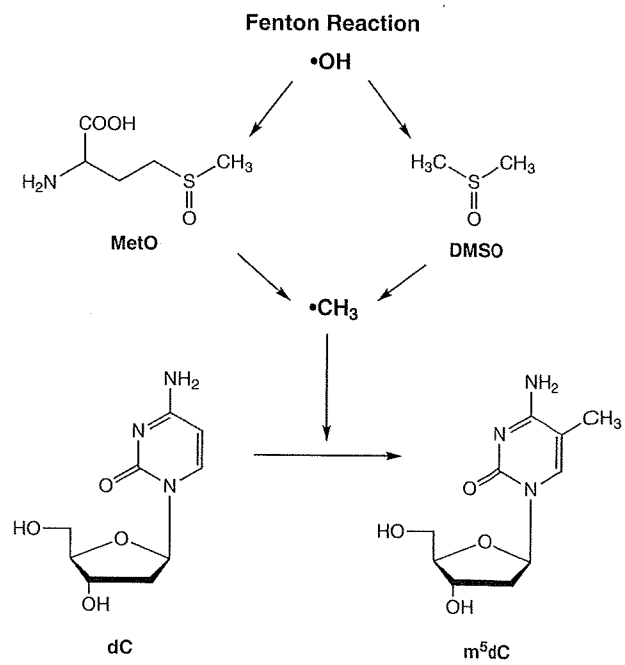

Scheme 1. Formation of m^5dC via methyl radicals by DMSO and MetO, triggered by Fenton reaction.

* Corresponding author. Tel.: +81 93 691 7469; fax: +81 93 601 2199.
E-mail address: h-kasai@med.uoeh-u.ac.jp (H. Kasai).

0960-894X/$ - see front matter © 2009 Elsevier Ltd. All rights reserved.
doi:10.1016/j.bmcl.2009.10.124

and high DNMT expression were also reported.[12,13] Therefore, it would be interesting to examine whether cytosine C-5 methylation via methyl radicals occurs by other biological/chemical systems.

Methyl radicals are reportedly generated by the reaction of OH radicals with dimethylsulfoxide (DMSO),[14] from the amino acid methionine (Met) upon gamma irradiation,[15] and by the treatment of methionine sulfoxide (MetO) with peroxynitrite.[16] Particularly, endogenous MetO formation in proteins is implicated as a pathological biomarker in relation to aging, inflammation and smoking.[17–20] It is worth mentioning that DNA hypermethylation during carcinogenesis is correlated to aging, inflammation and smoking.[21–23] DMSO also reportedly has an effect on the cellular epigenetic profile, by inducing DNA hypermethylation.[24] In this study, we examined the biological relevance of m^5dC formation in dC and DNA by methyl radicals produced from DMSO and MetO treated with a Fenton system (Scheme 1).

When dC was reacted with DMSO in the presence of Fenton reagent[8] at pH 7.3, the formation of m^5dC was clearly identified by HPLC equipped with a photodiode array UV detector (Fig. 1). The retention time and the UV spectrum of the reaction product were the same as those of the authentic m^5dC. Its formation was dependent on the concentration of DMSO (Fig. 2), and the reaction was rather rapid, due to its radical character. The reaction was approx-

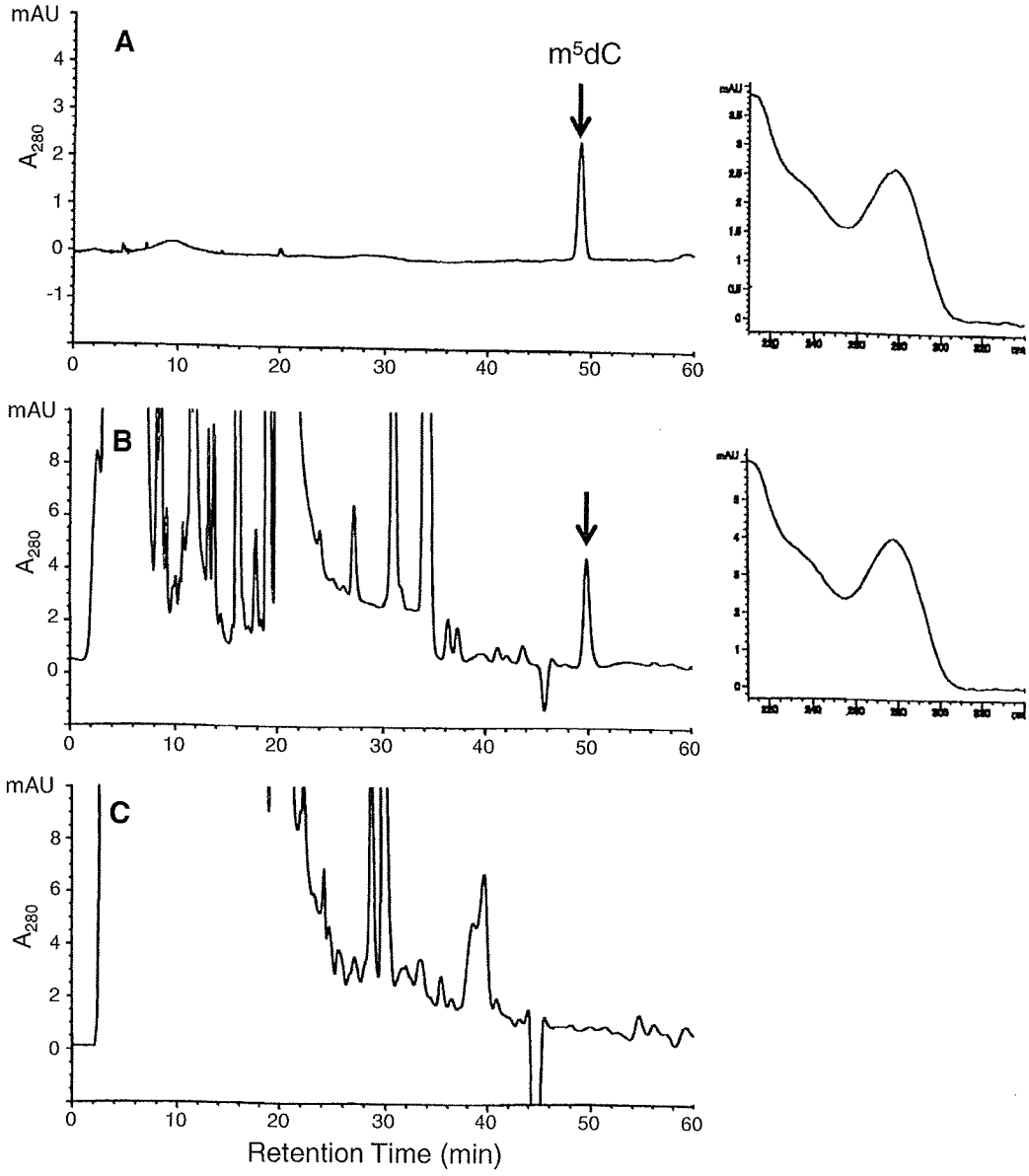

Figure 1. Detection of m^5dC in the reaction mixture of dC, DMSO and Fenton reagent by HPLC. The reaction mixture[8] (mixed under N_2 atmosphere, final volume, 0.225 ml), containing dC (final concentration, 5.46 mM), DMSO (100 mM), L-ascorbic acid (10.7 mM), EDTA-2Na (3.1 mM), $FeSO_4$ (5.3 mM), and H_2O_2 (19.6 mM) in 110 mM phosphate buffer (pH 7.3), was reacted in a sealed plastic tube (tube volume, 2 ml) by vigorous shaking at 37 °C. After a 3 h reaction, the solution was centrifuged and an aliquot of the supernatant was injected into the HPLC apparatus. (A) Chromatogram of the m^5dC standard (left) and its UV spectrum (right); (B) chromatogram of the reaction mixture (left) and UV spectrum of the peak at 50 min (right); (C) chromatogram of the control reaction mixture without DMSO.

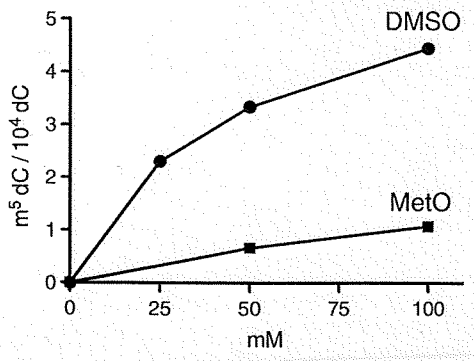

Figure 2. Dose-dependency of m^5dC formation in the dC/DMSO/Fenton reaction and the dC/MetO/Fenton reaction. The reaction conditions were the same as those in Figure 1, except that different concentrations of DMSO (25, 50 and 100 mM) and MetO (50 and 100 mM) were used. Mean values of duplicate experiments are plotted.

imately 65% complete within 5 min (data not shown). This reaction may proceed via a free radical mechanism, probably via a methyl radical. The dose-dependent formation of m^5dC from dC was also observed after a reaction with MetO plus Fenton reagent (Fig. 2).

In addition, after a double-stranded alternating copolymer, ds poly(dG-dC), was reacted with DMSO or MetO in the presence of Fenton reagent at pH 7.3, the formation of m^5dC was clearly detected in the poly(dG-dC) after the treatment, by an immuno-dot blot analysis[9,25] (Fig. 3). As a positive control, we analyzed 0.02–0.2 ng of calf thymus DNA, which contained 1.39 mol % m^5dC per P atoms. The chemiluminescence intensity increased depending upon the calf thymus DNA concentration. The control poly(dG-dC) without treatment also showed weak chemiluminescence. This means that commercial poly(dG-dC) contains a small amount of m^5dC. Since an exact quantitation was difficult with the immuno-dot blot analysis, the amount of m^5dC in the reaction mixture was further analyzed by the LC/MS/MS.

In the LC/MS analysis, the standard m^5dC exhibited an MH^+ ion at *m/z* 242, and product ion analysis from *m/z* 242 with

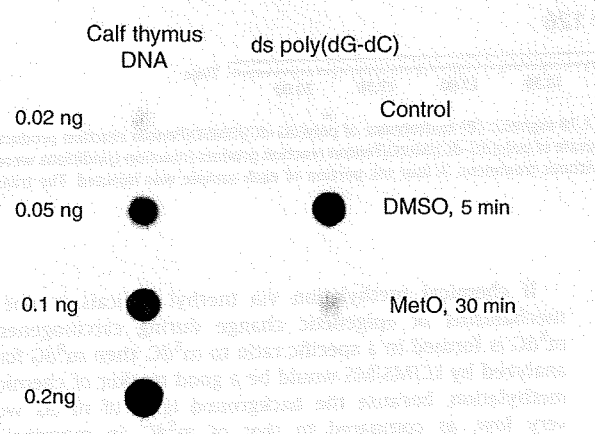

Figure 3. Detection of m^5dC in ds poly(dG-dC) by an immuno-dot blot analysis.[9,25] The reaction mixture (mixed under N_2 atmosphere, final volume, 0.45 ml) contained ds poly(dG-dC) (final concentration, 8.9 A_{260} OD units/ml), DMSO or MetO (100 mM), L-ascorbic acid (10.7 mM), EDTA·2Na (3.1 mM), $FeSO_4$ (5.3 mM), and H_2O_2 (19.6 mM), in 110 mM phosphate buffer (pH 7.3), and was reacted in a sealed plastic tube (tube volume, 2 mL) by vigorous shaking at 37 °C. After 5 min or 30 min, the ds poly(dG-dC) was recovered from the reaction mixture and was used for the analysis. As positive controls, m^5dC in various amounts of calf thymus DNA was visualized. As negative controls, untreated ds poly(dG-dC) was analyzed.

11 eV revealed a fragment BH_2^+ ion at *m/z* 126, formed by the loss of 2′-deoxyribose.[9] Therefore, the m^5dC in the reaction mixture was analyzed by LC/MS/MS, by monitoring the *m/z* 242→126 transition. In Figure 4, chromatograms of the LC/MS/MS analysis of standard m^5dC (A), poly(dG-dC)–DMSO–Fenton reagent (B), poly(dG-dC)–MetO–Fenton reagent (C), and control poly(dG-dC) without treatment (D) are shown. In both of the poly(dG-dC) samples treated with DMSO and MetO in the presence of Fenton reagent, a 242→126 transition peak appeared at 7.64 min, which is the same retention time as that of authentic m^5dC. The control poly(dG-dC) without treatment also showed a small peak (Fig. 4D). This means that the commercial poly(dG-dC) contains a small amount of m^5dC.

Based on the LC/MS/MS analysis, the yields of m^5dC in the DNA–DMSO–Fenton and DNA–MetO–Fenton reactions were calculated to be $5.00/10^4$ dC and $1.64/10^4$ dC, respectively, which are in the same range ($2–4/10^4$ dC) as the yield produced by the monomer reactions for 30 min with the DMSO- and MetO–Fenton reagents (data not shown). The high yield in DNA is unexpected, as compared to the previous result that showing the yield of m^5dC formation by a cumene hydroperoxide/Fe^{2+} system is 10-fold lower in DNA than in the dC monomer.[9] The following reasons are possible. (i) The Fenton system used in this study has higher affinity to DNA than to the monomer dC, thus generating higher levels of ·OH radicals in DNA;[26] (ii) long-range electron transfer along the DNA chain from the metal binding sites to the dC residues enhanced the yield of m^5dC in DNA.[27] Further studies with precise measurements of m^5dC using a stable isotope internal standard are required for the final conclusion.

We also analyzed the m^8dG in these reaction products by LC/MS/MS. The standard m^8dG[28] exhibited an MH^+ ion at *m/z* 282, and product ion analysis from *m/z* 282 revealed a fragment BH_2^+ ion at *m/z* 166, formed by the loss of 2′-deoxyribose. Therefore, the m^8dG was analyzed by monitoring the *m/z* 282→166 transition. In Figure 5, chromatograms of the LC/MS/MS analysis of standard m^8dG (A), poly(dG-dC)–DMSO–Fenton reagent (B), poly(dG-dC)–MetO–Fenton reagent (C), and control poly(dG-dC) without treatment (D) are shown. In the poly(dG-dC) treated with DMSO and MetO in the presence of Fenton reagent, a 282→166 transition peak appeared at 18.6 min (Fig. 5B and C), which is the same retention time as that of authentic m^8dG (Fig. 5A). The control poly(dG-dC) without treatment also displayed a small peak of m^8dG (Fig. 5D), which shows that the commercial poly(dG-dC) contains a small amount of m^8dG in addition to m^5dC. The formation of m^5dC and m^8dG in DNA polymers is summarized in Table 1. The yield of m^5dC formation in DNA was found to be 15–30-fold higher than that of m^8dG by the reaction with DMSO and MetO in the presence of Fenton reagent.

DMSO is known to induce hypermethylation of various genetic loci and affects the epigenetic profile in mouse embryoid bodies. Although those authors ascribed DNA methylation to the increase of DNMT3a activity,[24] other mechanisms of DNA methylation cannot be ruled out. DMSO also enhanced the invasiveness and metastatic potential of cultured epithelial cells, with an epigenetic effect.[29]

DNA hypermethylation is increased with age, inflammation and smoking.[21–23] The MetO/Met ratio in proteins also reportedly increased with age, inflammation and smoking.[17–20] MetO in proteins is repaired by methionine sulfoxide reductase (Msr). Three reports have suggested that the Msr gene is a tumor suppressor.[30–32]

The chemical methylation of cytosine C-5 may occur in vivo. A Met residue in a chromatin protein reportedly interacts with DNA by the intercalation of the Met side chain into a GC pair, based on NMR studies.[33] If the Met residue is oxidized to MetO, then the cytosine residues in the vicinity could undergo C-5 methylation

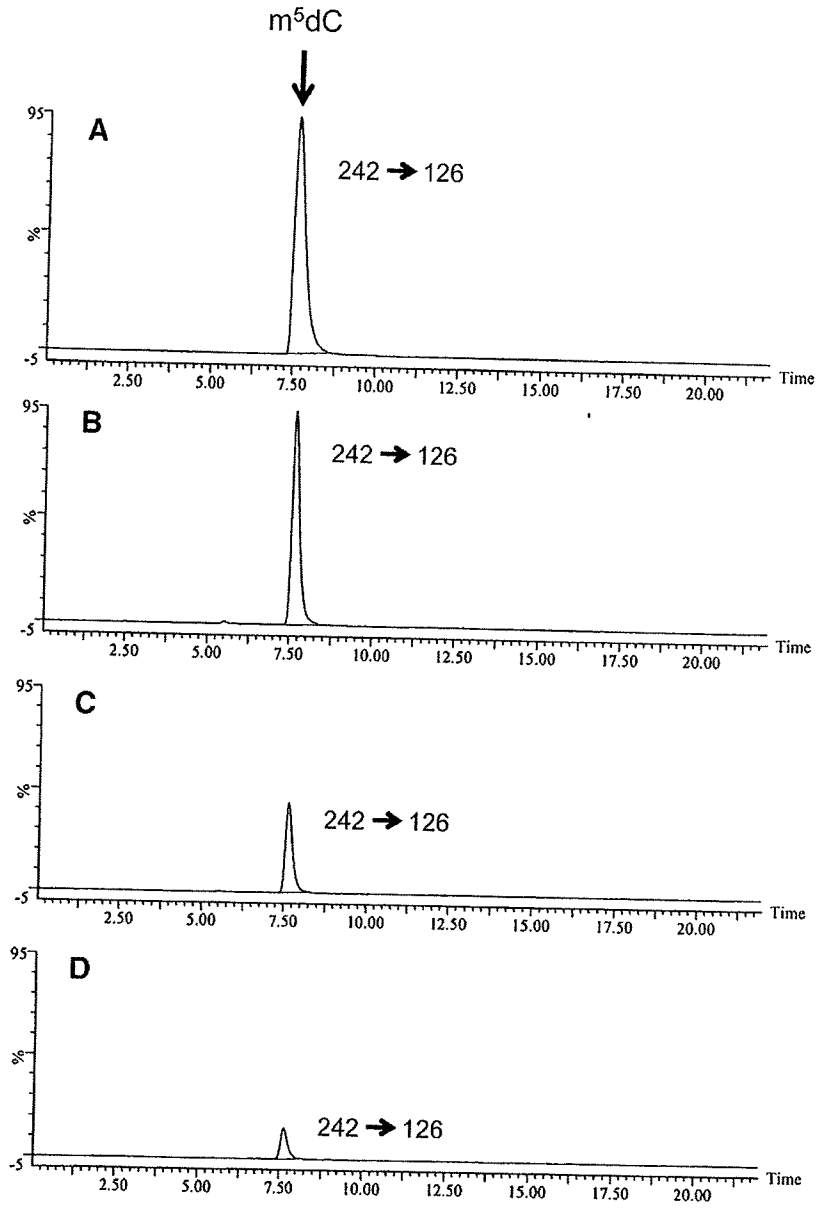

Figure 4. LC/MS/MS analysis of m^5dC in the reaction products. (A) Standard m^5dC (1.78 mg/mL); (B) hydrolysate of poly(dG-dC)/DMSO/Fenton reaction product (reaction conditions were the same as those in Figure 3, with 30 min reaction time); (C) hydrolysate of poly(dG-dC)/MetO/Fenton reaction product (reaction conditions were the same as those in Figure 3, with 30 min reaction time); and (D) control ds poly(dG-dC) without treatment. A four mL portion of each sample was injected. The transition *m/z* 242→126 was monitored. Chromatograms B, C and D are shown on the same scale.

when triggered by ·OH radicals. Various oxidized proteins and their degradation products may accumulate in the cytosol during aging and inflammation and may react with dCTP to form m^5dCTP, which could become incorporated into DNA and induce gene silencing.[34]

In the present study, in addition to m^5dC, the formation of a small amount of m^8dG was detected in the poly(dG-dC) after the treatment. The higher level of m^5dC formation than that of m^8dG may be due to a steric effect. Namely, the cytosine C-5 position may be present in a more open structure in the DNA, while the guanine C-8 is sterically hindered by the phosphate backbone.

If chemical methylation via methyl radicals is one of the mechanisms of epigenetic change during carcinogenesis, and m^8dG is formed in a specific ratio to m^5dC, then m^8dG formation analyzed by LC/MS/MS would be a good marker of chemical DNA methylation, because the background level of m^8dG would be very low, as compared to that of m^5dC, in mammalian cell DNA. Therefore, epi-mutagens inducing DNA hypermethylation can be assayed by in vitro experiments using cultured cells. The analysis of the accumulation status of m^8dG in human DNA may also be a good indicator of the increase of m^5dC in DNA by radical mechanisms, and would be useful for human cancer risk assessment.

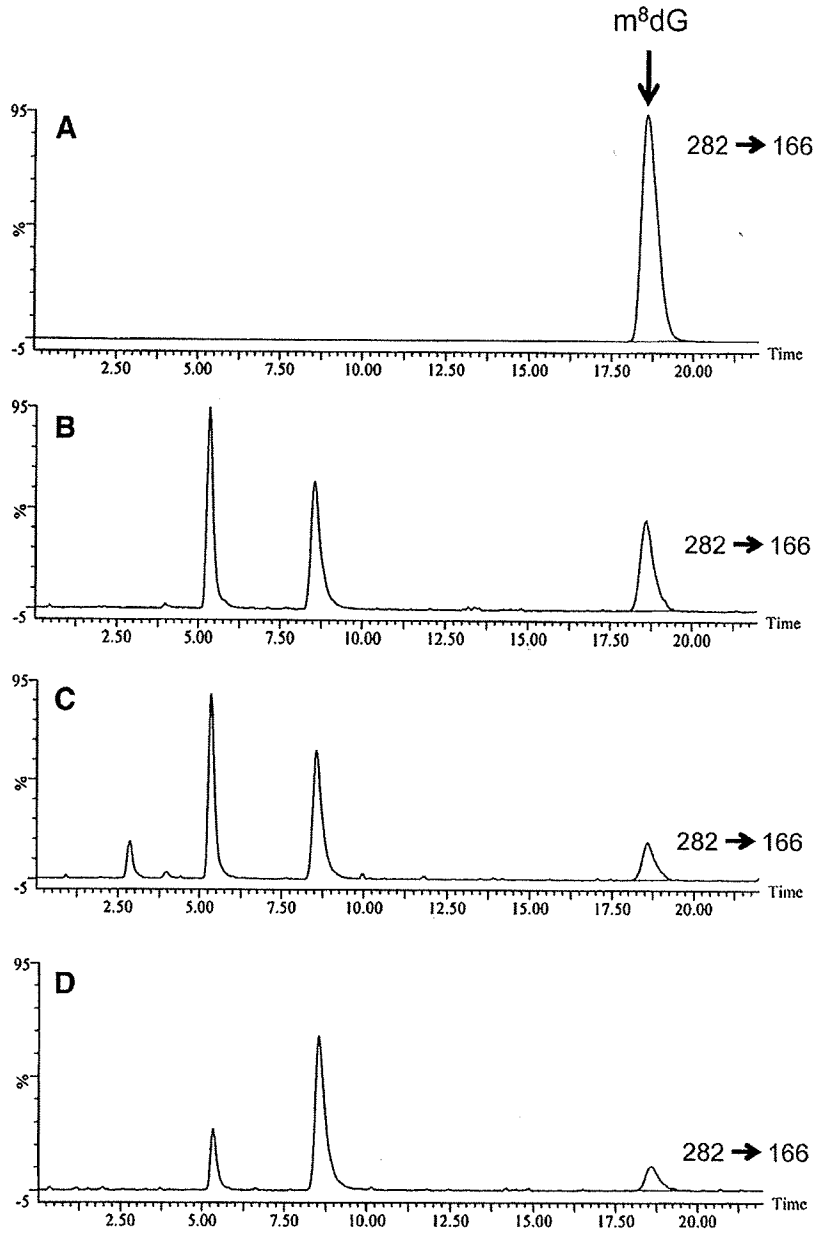

Figure 5. LC/MS/MS analysis of m^8dG in the reaction products. (A) Standard m^8dG[28] (2.08 μg/mL); (B, C, D) the same samples as B, C, D in Figure 4.

Table 1
Formation of m^5dC and m^8dG in ds poly(dG-dC) by DMSO and MetO in the presence of Fenton reagent

Reaction	$m^5dC/10^4$ dC	$m^8dG/10^4$ dG
DMSO + Fenton reagent	5.00	0.27
MetO + Fenton reagent	1.64	0.06

Acknowledgments

This work was supported by grants from the Ministry of Health, Labor and Welfare of Japan, and a grant from Asia International Educational Program for Graduate Students in the Field of Occupational Health.

References and notes

1. Taffe, B. G.; Takahashi, N.; Kensler, T. W.; Mason, R. P. *J. Biol. Chem.* **1987**, *262*, 12143.
2. Augusto, O.; Du Plessis, L. R.; Weingrill, C. L. *Biochem. Biophys. Res. Commun.* **1985**, *126*, 853.
3. Goria-Gatti, L.; Iannone, A.; Tomasi, A.; Poli, G.; Albano, E. *Carcinogenesis* **1992**, *13*, 799.
4. Nakao, L. S.; Kadiiska, M. B.; Mason, R. P.; Grijalba, M. T.; Augusto, O. *Free Radical Biol. Med.* **2000**, *29*, 721.
5. Nakao, L. S.; Ouchi, D.; Augusto, O. *Chem. Res. Toxicol.* **1999**, *12*, 1010.
6. Hix, S.; Morais Mda, S.; Augusto, O. *Free Radical Biol. Med.* **1995**, *19*, 293.
7. Netto, L. E.; RamaKrishna, N. V.; Kolar, C.; Cavalieri, E. L.; Rogan, E. G.; Lawson, T. A.; Augusto, O. *J. Biol. Chem.* **1992**, *267*, 21524.
8. Kang, J. O.; Gallagher, K. S.; Cohen, G. *Arch Biochem. Biophys.* **1993**, *306*, 178.
9. Kasai, H.; Kawai, K. *Chem. Res. Toxicol.* **2009**, *22*, 984.
10. Benbrahim-Tallaa, L.; Waterland, R. A.; Dill, A. L.; Webber, M. M.; Waalkes, M. P. *Environ. Health Perspect.* **2007**, *115*, 1454.

11. Robertson, K. D.; Uzvolgyi, E.; Liang, G.; Talmadge, C.; Sumegi, J.; Gonzales, F. A.; Jones, P. A. *Nucleic Acids Res.* **1999**, *27*, 2291.
12. Eads, C. A.; Danenberg, K. D.; Kawakami, K.; Saltz, L. B.; Danenberg, P. V.; Laird, P. W. *Cancer Res.* **1999**, *59*, 2302.
13. Ehrlich, M.; Woods, C. B.; Yu, M. C.; Dubeau, L.; Yang, F.; Campan, M.; Weisenberger, D. J.; Long, T.; Youn, B.; Fiala, E. S.; Laird, P. W. *Oncogene* **2006**, *25*, 2636.
14. Eberhardt, M. K.; Colina, R. *J. Org. Chem.* **1988**, *53*, 1071.
15. Makino, K. *J. Phys. Chem.* **1979**, *83*, 2520.
16. Nakao, L. S.; Iwai, L. K.; Kalil, J.; Augusto, O. *FEBS Lett.* **2003**, *547*, 87.
17. Wells-Knecht, M. C.; Lyons, T. J.; McCance, D. R.; Thorpe, S. R.; Baynes, J. W. *J. Clin. Invest.* **1997**, *100*, 839.
18. Onorato, J. M.; Thorpe, S. R.; Baynes, J. W. *Ann. N.Y. Acad. Sci.* **1998**, *854*, 277.
19. Hosako, M.; Ogino, T.; Omori, M.; Okada, S. *Free Radical Biol. Med.* **2004**, *36*, 112.
20. Carp, H.; Miller, F.; Hoidal, J. R.; Janoff, A. *Proc. Natl. Acad. Sci. U.S.A.* **1982**, *79*, 2041.
21. Kim, S. K.; Jang, H. R.; Kim, J. H.; Kim, M.; Noh, S. M.; Song, K. S.; Kang, G. H.; Kim, H. J.; Kim, S. Y.; Yoo, H. S.; Kim, Y. S. *Carcinogenesis* **2008**, *29*, 1623.
22. Suzuki, H.; Toyota, M.; Kondo, Y.; Shinomura, Y. *Methods Mol. Biol.* **2009**, *512*, 55.
23. Kim, J. S.; Kim, H.; Shim, Y. M.; Han, J.; Park, J.; Kim, D. H. *Carcinogenesis* **2004**, *25*, 2165.
24. Iwatani, M.; Ikegami, K.; Kremenska, Y.; Hattori, N.; Tanaka, S.; Yagi, S.; Shiota, K. *Stem Cells* **2006**, *24*, 2549.
25. Leuratti, C.; Singh, R.; Lagneau, C.; Farmer, P. B.; Plastaras, J. P.; Marnett, L. J.; Shuker, D. E. *Carcinogenesis* **1998**, *19*, 1919.
26. Floyd, R. A. *Biochem. Biophys. Res. Commun.* **1981**, *99*, 1209.
27. Arkin, M. R.; Stemp, E. D.; Pulver, S. C.; Barton, J. K. *Chem. Biol.* **1997**, *4*, 389.
28. Maeda, M.; Nushi, K.; Kawazoe, Y. *Tetrahedron* **1974**, *30*, 2677.
29. Bentel, J. M.; Rhodes, G. C.; Markus, I.; Smith, G. J. *Int. J. Cancer* **1990**, *46*, 251.
30. Bilsborough, J.; Van Pel, A.; Uyttenhove, C.; Boon, T.; Van den Eynde, B. J. *J. Immunol.* **1999**, *162*, 3534.
31. Lei, K. F.; Wang, Y. F.; Zhu, X. Q.; Lu, P. C.; Sun, B. S.; Jia, H. L.; Ren, N.; Ye, Q. H.; Sun, H. C.; Wang, L.; Tang, Z. Y.; Qin, L. X. *BMC Cancer* **2007**, *7*, 172.
32. De Luca, A.; Sacchetta, P.; Nieddu, M.; Di Ilio, C.; Favaloro, B. *BMC Mol. Biol.* **2007**, *8*, 39.
33. Allain, F. H.; Yen, Y. M.; Masse, J. E.; Schultze, P.; Dieckmann, T.; Johnson, R. C.; Feigon, J. *EMBO J.* **1999**, *18*, 2563.
34. Holliday, R.; Ho, T. *Somat. Cell Mol. Genet.* **1991**, *17*, 537.

Cancer Science
The official journal of the Japanese Cancer Association JCA

Body iron store as a predictor of oxidative DNA damage in healthy men and women

Ai Hori,[1,2,6] Tetsuya Mizoue,[1] Hiroshi Kasai,[3] Kazuaki Kawai,[3] Yumi Matsushita,[1] Akiko Nanri,[1] Masao Sato[4] and Masanori Ohta[5]

[1]Department of Epidemiology and International Health, Research Institute, International Medical Center of Japan, Tokyo; [2]Department of Microbiology, University of Occupational and Environmental Health, Kitakyushu; [3]Institute of Industrial Ecological Sciences, Department of Environmental Oncology, University of Occupational and Environmental Health, Kitakyushu; [4]Department of Applied Biological Chemistry, Graduate School of Bioresource and Bioenvironmental Sciences, Kyusyu University, Fukuoka; [5]Department of Health Development, University of Occupational and Environmental Health, Kitakyushu, Japan

(Received July 1, 2009/Revised September 30, 2009/Accepted October 4, 2009/Online publication November 5, 2009)

While iron plays an important role in many cellular functions, excess iron storage induces DNA damage by generating hydroxyl radicals and thus promotes carcinogenesis. However, it remains unclear whether body iron levels that are commonly observed in a general population are related to oxidative DNA damage. We examined the association between serum ferritin concentrations and levels of urinary 8-hydroxydeoxyguanosine (8-OHdG), a biomarker of systemic oxidative DNA damage and repair, in 528 Japanese men and women aged 21–67 years. Men had much higher ferritin levels than in women, and the levels were significantly greater in women aged 50 years or older than in women aged less than 50 years. Urinary 8-OHdG concentrations were significantly and positively associated with serum ferritin levels in all the subgroups. The Spearman rank correlation coefficients were 0.47, 0.76, and 0.73 for men overall, women aged less than 50 years, and women aged 50 years or older, respectively. These associations were materially unchanged after adjustment for potential confounding variables. In men, a more pronounced association was observed in nonsmokers than in smokers. Our results suggest body iron storage is a strong determinant of levels of systemic oxidative DNA damage in a healthy population. (*Cancer Sci* 2010; 101: 517–522)

Iron plays an important role in cellular metabolism and aerobic respiration. In healthy adults, 1 to 2 mg of dietary iron is absorbed a day, and body iron is distributed between blood (~3000 mg, mostly as hemoglobin), liver (~1000 mg, mostly as ferritin), skeletal muscle (~300 mg), and macrophages (~600 mg).[1] Besides, iron generates hydroxyl radicals according to the Fenton reaction *in vivo*,[2] and thus has been hypothesized to promote carcinogenesis through lipid peroxidation and oxidative DNA and protein damage.[3] In experimental animals,[4] excess intake of heme iron induces the formation of radicals and the occurrence of colon cancer. In humans, high dietary intake of heme iron[5,6] and blood measurements of iron[7–10] have been shown to be associated with an increased risk of cancer. More recently, a randomized control trial found that phlebotomy, accompanied by a considerable reduction in serum ferritin levels, significantly decreased risk of cancer in men with a peripheral arterial disease.[11] Such evidence suggests that cancer risk may vary according to body iron status even at levels commonly observed among the general population who do not have iron metabolic disorders. However, epidemiologic evidence regarding iron and cancer is far from consistent[12,13] and the finding from the above-mentioned trial should be interpreted cautiously because cancer was not the primary outcome.[14] Investigations linking body iron to biomarkers of carcinogenesis may provide data to support or refute whether iron level currently admitted as normal influences cancer risk.

Urinary 8-hydroxydeoxyguanosine (8-OHdG) is a reliable biomarker of systemic oxidative DNA damage.[2] Further, epidemiologic studies have shown that urinary 8-OHdG concentrations can predict cancer risk.[15–17] However, few studies have been performed to quantitate 8-OHdG levels in association with body iron status. Nakano *et al.* reported a positive correlation between serum ferritin concentrations and urinary 8-OHdG levels in 2507 healthy men and women.[18] However, they did not control for smoking and body mass index, factors known to be associated with 8-OHdG levels.[19,20] In a small study of 48 mild dyslipidemic men, Tuomainen *et al.* demonstrated a linear, positive relationship between serum ferritin and urinary 8-OHdG with adjustment for smoking, body mass index, and physical activity.[21] To further explore this issue, the present study examined the association between serum ferritin concentrations, a marker of body iron storage[22] and urinary 8-OHdG levels in healthy men and women while adjusting for potential confounding factors.

Materials and Methods

Study participants. In 2006, a health survey was conducted among employees of two municipal offices in north-eastern Kyushu, Japan.[23] At the time of routine health check-up, all full-time workers (n = 601) except those on long sick-leave or maternity-leave were invited; of these, 547 subjects (323 men and 224 women aged 21–67 years) participated (response rate, 91%). Prior to the examination, participants completed a questionnaire on lifestyle including smoking, alcohol drinking, diet, and exercise, which was then checked by research staff for completeness and, where necessary, clarified by asking the subject. Participants were also asked to donate blood and urine specimens. We excluded 13 subjects with missing information on 8-OHdG and ferritin concentrations, body mass index, and smoking status. Furthermore, those who reported they had cancer (one with thyroid cancer and two with breast cancer) or other diseases that affect serum ferritin levels (one with anemia and two with chronic liver disorder) were also excluded. Finally, 528 subjects (313 men and 215 women) remained for the present analyses. The ethics committee of the International Medical Center of Japan approved the protocol of the study, and written informed consent was obtained from each participant.

Measurement of urinary 8-OHdG. Urinary 8-OHdG and creatinine were determined by a method previously described.[24] In short, a human urine sample was mixed with the same volume of a dilution solution containing the ribonucleoside marker 8-hydroxyguanosine. A 20-μL aliquot of the diluted urine sample

[6]To whom correspondence should be addressed.
E-mail: ihori-sgy@umin.ac.jp

doi: 10.1111/j.1349-7006.2009.01394.x

was injected into HPLC-1 (MCI GEL CA08F, 7 μm, 1.5 × 120 mm; elution, 2% acetonitrile in 0.3 mM sulfuric acid, 50 μL/min, 65°C), via the guard column (1.5 × 40 mm), and the chromatograms were recorded by a Gilson UV detector (UV/VIS-155 with 0.2 mm light path cell). Creatinine was detected at 245 nm. The 8-OHdG fraction was collected, depending on the relative elution position from the peak of the added marker, 8-hydroxyguanosine, and was automatically injected into the HPLC-2 column. The 8-OHdG fraction was fractionated by the HPLC-2 column (Capcell Pak C18, Shiseido, Tokyo, Japan; 5 μm, 4.6 × 250 mm; elution, 10 mM sodium phosphate buffer [pH 6.7] containing 5% methanol and an antiseptic Reagent MB [100 μL/L], 1 mL/min, 40°C). The 8-OHdG was detected by a Coulochem II EC detector (ESA, Chelmsford, MA, USA) with a guard cell (5020) and an analytical cell (5011) (applied voltage: guard cell, 350 mV; E1, 170 mV; E2, 300 mV). The accuracy of the measurement, estimated from the recovery of an added 8-OHdG standard, was 90–98%. When the same urine sample was analyzed three times, the variation of the data was within 7%. 8-OHdG levels were adjusted for urinary creatinine levels before statistical analysis.

Measurement of serum ferritin. From each individual, 9 mL of venous blood was drawn in a vacuum blood collection tube and carried to our laboratory in a cooled box. Blood was centrifuged for 15 min and the serum separated was stored in a maximum of six tubes (0.5 mL each) at −20°C until analysis. Serum ferritin concentrations were measured by chemiluminescence immunoassay on the Bayer ADVIA Centaur at an external laboratory (Mitsubishi Chemical Medicine, Tokyo, Japan).

Other variables. Body height was measured to the nearest 0.1 cm with the subject standing without shoes. Body weight in light clothes was measured to the nearest 0.1 kg. Body mass index (BMI) was calculated as the body weight (kg) divided by the square of body height (m). Smoking status and alcohol intake were self-reported in the lifestyle questionnaire. Participants were asked about weekly hours of leisure-time physical activity engaged in for each of the four activities: strolling or walking; mild exercise; moderate intensity exercise; strong intensity exercise. Weekly minutes for walking or cycling while commuting to and from the work were also ascertained. Average metabolic equivalent task (MET) values were assigned to each level of activity according to the intensity of exercise, and total MET-hours per week was estimated by summing all of the values for each participant. Dietary habit for the preceding month was assessed with a brief self-administered diet history questionnaire.[25] Intakes of iron, vitamin C, and vitamin E were estimated by an ad hoc computer algorithm, and their energy-adjusted values (per 1000 kcal) were used for analysis. Blood hemoglobin was measured by sodium lauryl sulfate–hemoglobin method, serum iron was determined by colorimetric assay, and red blood cells were counted by automated blood counting machine at an external laboratory.

Statistical analysis. Median and inter-quartile range of serum ferritin, urinary 8-OHdG, and blood hemoglobin concentrations were calculated according to age (<35, 35–49, or ≥50 years), smoking status (nonsmoker, quitter, smoking 1–19 cigarettes/day, or smoking ≥20 cigarettes/day), BMI (tertile), ethanol consumption (0, 0.1–19.9, 20–39.9, or ≥40 g/day), physical activity (0, 0.1–4.9, 5–9.9, or ≥10 MET-h/week), vitamin C (tertile), and vitamin E (tertile), and the difference between groups was assessed using the Wilcoxon two-sample test. The Spearman rank correlation coefficient was calculated to assess the association between serum ferritin and urinary 8-OHdG concentrations. In women, because serum ferritin concentrations considerably increase after menopause,[26] analyses were done separately for those aged less than 50 years, and 50 years or older, with reference to data regarding the mean age of menopause in Japanese women (48.3 years old).[27]

Both ferritin and 8-OHdG concentrations were log-transformed for the following parametric analyses. The geometric mean and its 95% confidence interval of urinary 8-OHdG concentrations were calculated for each tertile of the serum ferritin levels for the three groups: men, women aged less than 50 years, and women aged 50 years or older. To control the effects of potential confounding variables, we performed three types of analysis. In Model 1, we adjusted for age (continuous), smoking status (nonsmoker or smoker), and BMI (continuous). In Model 2, we additionally adjusted for hemoglobin levels (continuous). In Model 3, we adjusted for alcohol consumption (0, 0.1–19.9, 20–39.9, or ≥40 g/day), physical activity (0, 0.1–4.9, 5–9.9, or ≥10 MET-h/week), vitamin C intake (tertile), and vitamin E intake (tertile) in addition to the covariates in Model 1. Trend association was evaluated by assigning 1–3 to the lowest through highest tertile categories of ferritin concentrations. Because smoking is a known, consistent determinant of urinary 8-OHdG concentrations,[28] analysis was repeated by smoking status in men. Statistical tests were two-sided and regarded as statistically significant at P-value <0.05. Analysis was done with STATA SE version 10.0 (Lakeway Drive College Station, TX, USA).

Results

Table 1 presents medians of urinary 8-OHdG and serum ferritin concentrations according to age, smoking, and BMI for women and men. There was no significant difference in 8-OHdG concentration between women and men (2.95 *vs* 3.10 μg/g creatinine, $P = 0.45$), although women showed a greater variation of 8-OHdG concentrations than did men. In women, those aged 50 years or older had significantly higher 8-OHdG levels than those aged less than 50 years (3.35 *vs* 2.90, $P = 0.043$). Median serum ferritin concentration markedly differed among the three groups ($P < 0.001$): 24.9, 51.2, and 130 ng/mL for women under 50 years, women aged 50 years or older, and men, respectively. In men, smokers had significantly higher 8-OHdG ($P < 0.001$) and ferritin concentrations ($P = 0.042$) than nonsmokers. Blood hemoglobin levels did not appreciably differ according to demographic and lifestyle factors except smoking; heavy smokers showed a higher mean of hemoglobin levels than nonsmokers in men. In both women and men, ferritin concentrations tended to increase with BMI. In men, 8-OHdG levels decreased as BMI increased (P for trend = 0.01) but tended to increase with increasing intake of vitamin C. In women, both serum ferritin and 8-OHdG levels were significantly higher in the highest category of vitamin C intake or physical activity than in the lowest category of the respective variable.

Serum ferritin concentrations were significantly and positively correlated with urinary 8-OHdG concentrations in both women and men (Fig. 1), with the Spearman rank correlation coefficient being 0.47, 0.76, and 0.73 for men, women aged less than 50 years, and women aged 50 years or older, respectively. In men, the coefficient was 0.52, 0.52, 0.45, and 0.31 for nonsmokers, quitters, 1–19 cigarettes/day, and 20 or more cigarettes/day, respectively. Meanwhile, regression coefficients of log-transformed ferritin (ng/mL) on log-transformed 8-OHdG (μg/g creatinine) were 0.748, 0.737, and 0.546, for women under 50 years, women aged 50 years or older, and men, respectively.

As Table 2 shows, the geometric mean of urinary 8-OHdG concentrations increased steadily as serum ferritin levels increased in all the three groups (P for trend <0.001), and this association was materially unchanged after adjustment of potential confounders. Of all the subgroups divided by sex, age, and serum ferritin levels, the highest unadjusted geometric mean of 8-OHdG concentrations was recorded in the highest tertile of ferritin among women aged 50 years or older (4.87 μg/g creatinine), whereas the lowest mean was observed in the lowest

doi: 10.1111/j.1349-7006.2009.01394.x

Table 1. Description of study participants (n = 528)

	n	Urinary 8-OHdG concentrations (μg/g creatinine)	Serum ferritin concentrations (ng/mL)	n	Blood hemoglobin levels (g/dL)†
Women (n = 215)					
Age (years)					
<35	72	2.84 (2.17–3.85)	24.4 (12.3–44.3)	72	13.2 (12.5–14.0)
35–49	82	3.09 (2.04–4.03)	25.5 (12.5–54.8)	82	13.2 (12.7–13.6)
≥50	61	3.35 (2.37–4.84)	51.2 (20.8–119.0)**	61	13.3 (12.8–14.1)
Smoking					
Nonsmoker	208	2.99 (2.20–4.20)	28.9 (14.0–56.9)	208	13.2 (12.7–13.8)
Quitter	3	2.75 (2.58–2.77)	24.0 (11.8–57.5)	3	13.1 (12.7–14.4)
Current smoker	4	2.76 (1.76–5.60)	24.3 (9.1–82.3)	4	14.3 (13.4–15.2)
BMI (kg/m^2)					
<18.5	46	2.64 (2.10–3.43)	22.5 (11.6–46.6)	46	13.1 (12.5–13.9)
18.5–21.9	106	3.13 (2.32–4.22)	29.1 (16.4–54.9)	106	13.1 (12.5–13.6)
≥22	63	3.05 (2.15–4.42)	35.5 (13.8–93.7)	63	13.5 (12.9–14.1)
Alcohol (ethanol consumption, g/day)					
0	69	2.91 (2.12–4.42)	29.3 (10.9–57.3)	69	13.1 (12.4–14.0)
0.1–19.9	131	2.95 (2.20–4.00)	27.9 (13.9–56.4)	131	13.2 (12.7–13.7)
20–39.9	15	3.07 (2.83–3.95)	32.7 (19.7–129.0)	15	13.6 (12.8–14.0)
Physical activity involved in leisure time exercise and commuting (MET-h/week)					
0	110	2.90 (2.20–4.07)	29.1 (13.9–52.7)	110	13.2 (12.7–13.9)
0.1–4.9	64	3.13 (2.17–4.02)	29.1 (14.3–68.7)	64	13.2 (12.7–13.8)
5–9.9	23	2.82 (2.26–3.95)	19.8 (10.0–43.9)	23	13.0 (12.1–13.8)
≥10	17	3.16 (2.76–4.59)	67.2 (20.8–115.0)*	17	13.4 (12.8–13.6)
Vitamin C consumption (mg/1000 kcal)‡					
<62	71	2.89 (2.39–3.80)	29.3 (13.8–52.7)	71	13.1 (12.4–13.6)
62–83.9	70	2.74 (1.89–4.06)	21.2 (8.9–44.0)	70	13.1 (12.5–13.7)
≥84	72	3.22 (2.31–4.40)	40.8 (21.2–101.1)**	72	13.4 (12.9–14.0)
Vitamin E consumption (mg/1000 kcal)					
<4.13	72	2.84 (2.06–3.80)	27.6 (12.2–52.1)	72	13.1 (12.4–14.0)
4.13–4.949	71	3.10 (2.15–4.18)	29.3 (14.7–57.3)	71	13.2 (12.7–13.8)
≥4.95	70	3.09 (2.29–4.26)	29.8 (13.9–79.4)	70	13.2 (12.7–13.8)
Men (n = 313)					
Age (years)					
<35	76	3.19 (2.55–3.86)	130.5 (78.4–191.0)	57	15.5 (15.1–16.1)
35–49	111	3.33 (2.41–4.28)	139.0 (90.2–232.0)	111	15.6 (15.1–16.2)
≥50	126	3.05 (2.43–3.72)	124.0 (75.7–196.0)	126	15.3 (14.8–16.1)
Smoking (cigarettes/day)					
Nonsmoker	113	2.92 (2.24–3.92)	120.0 (71.0–205.0)	102	15.4 (14.9–16.0)
Quitter	62	3.00 (2.37–3.60)	124.5 (83.3–181.0)	59	15.4 (14.9–15.9)
1–19	43	3.30 (2.79–4.27)*	128.0 (74.6–188.0)	38	15.4 (14.9–16.2)
≥20	95	3.38 (2.71–4.19)**	153.0 (93.0–249.0)*	95	15.7 (15.0–16.3)*
BMI(kg/m^2)					
<22	110	3.36 (2.63–4.12)	113.0 (79.2–184.0)	97	15.5 (14.9–16.1)
22–24.9	102	3.16 (2.43–3.96)	135.0 (78.0–198.0)	100	15.3 (14.9–16.0)
≥25	101	2.97 (2.35–3.77)*	156.0 (84.3–261.0)*	97	15.6 (14.9–16.2)
Alcohol (ethanol consumption, g/day)					
0	44	2.95 (2.33–3.78)	112.0 (65.5–183.0)	42	15.5 (14.9–16.1)
0.1–19.9	166	3.09 (2.52–4.14)	135.0 (78.4–195.0)	154	15.5 (14.9–16.1)
20–39.9	71	3.29 (2.43–3.96)	134.0 (98.1–249.0)*	67	15.4 (14.9–16.3)
≥40	32	3.24 (2.47–3.77)	135.0 (92.9–233.0)*	31	15.7 (15.3–16.3)
Physical activity involved in leisure time exercise and commuting (MET-h/week)					
0	108	3.32 (2.47–3.99)	131.5 (85.3–210.0)	101	15.5 (15.0–16.2)
0.1–4.9	82	2.89 (2.41–4.16)	143.5 (83.9–206.0)	79	15.6 (14.9–16.2)
5–9.9	42	3.01 (2.48–3.54)	146.0 (78.1–280.0)	40	15.6 (14.8–16.3)
≥10	79	3.19 (2.29–4.14)	120.0 (76.0–186.0)	72	15.3 (14.8–16.1)
Vitamin C consumption (mg/1000 kcal)‡					
<41	100	3.06 (2.40–3.67)	121.0 (83.5–189.0)	93	15.5 (14.9–16.1)
41–59.9	102	3.00 (2.37–3.90)	135.0 (88.4–211.0)	99	15.4 (14.9–16.3)
≥60	108	3.32 (2.60–4.18)*	134.0 (76.4–214.0)	99	15.5 (15.0–16.1)
Vitamin E consumption (mg/1000 kcal)					
<3.42	102	3.18 (2.42–3.90)	125.0 (83.7–212.0)	97	15.6 (14.9–16.2)
3.42–4.119	103	3.05 (2.43–4.06)	127.0 (83.6–187.0)	94	15.5 (15.0–16.2)
≥4.12	105	3.13 (2.50–3.99)	139.0 (76.0–224.0)	100	15.5 (14.9–16.0)

Values are median (inter-quartile range) unless otherwise stated. *P < 0.05, **P < 0.01 as compared with those in the lowest tertile (age, BMI, alcohol, physical activity, vitamin C and E) or with nonsmokers (smoking). †Blood hemoglobin has 19 missing values for men less than 35 years old. ‡Vitamin C and vitamin E have two missing values for women and three missing values in men. 8-OHdG, 8-hydroxydeoxyguanosine; BMI, body mass index; MET, metabolic equivalent task.

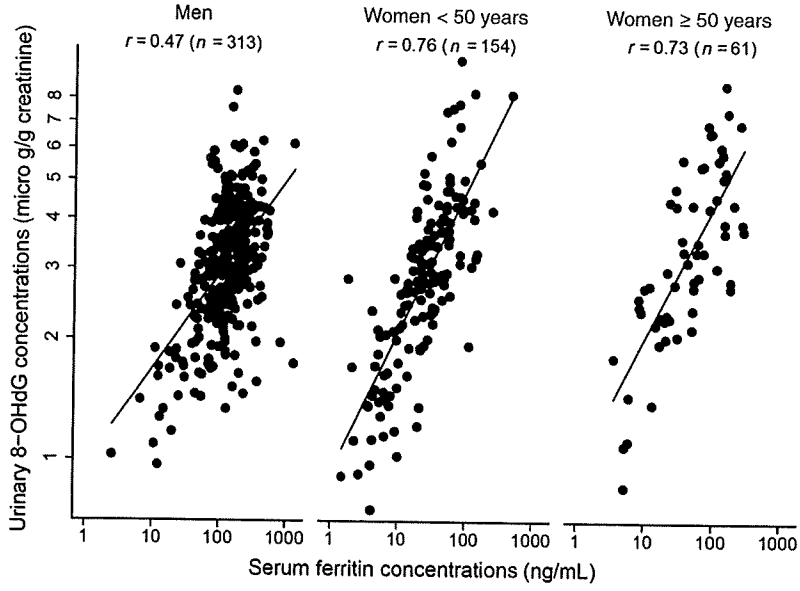

Fig. 1. Correlation between serum ferritin and urinary 8-hydroxydeoxyguanosine (8-OHdG) concentrations.

tertile of ferritin among women aged less than 50 years (1.80 μg/g creatinine). Urinary 8-OHdG concentrations were not significantly associated with red blood cell count, dietary iron intake, and serum iron concentrations (data not shown).

Discussion

In this cross-sectional biomarker study of healthy Japanese men and women, we found a strong positive association between serum ferritin and urinary 8-OHdG concentrations. This association was robust in all the subgroups whose serum ferritin concentrations markedly differed, and were materially unchanged even after adjustment for potential confounding variables. Our finding underscores the importance of body iron store as a determinant of level of oxidative DNA damage in a population without iron metabolism disorders.

8-OHdG, an oxidized nucleoside of DNA, is the most frequently detected DNA lesion in nuclear and mitochondrial DNA. Several reactive oxygen species, such as hydroxyl radical and singlet oxygen, attack on C-8 of guanine in DNA and generate 8-OHdG. 8-OHdG and its oxidation products lead to GC → TA transversions in human cells since 8-hydroxyguanine has hydrogen-bonding ability to adenine.[3] Base excision repair by 8-hydroxyguanine glycosylase1 is the major removal path of 8-OHdG from DNA.[1] Removed 8-OHdG from the whole body is excreted in human urine,[29] and thus urinary 8-OHdG is considered to reflect oxidative DNA damage and repair from all cells in the organism.

Ferritin is an iron binding protein that can store up to 4500 Fe^{3+}ions and is distributed throughout the body, and its concentrations in serum reflect the body's iron store.[30] Although ferritin itself has the potential to protect against oxidative stress by chelating free iron,[31] it could also act as a mediator of oxidative stress by releasing free iron.[32] This paradoxical behavior makes the role of ferritin in oxidative stress controversial.[33]

Previously, two studies have examined the association between serum ferritin and 8-OHdG concentrations in persons with no known condition that might influence these measurements. In a study of mild dyslipidemic men,[21] there was a significant positive association between the two measures (Spearman rank correlation coefficient, 0.36). However, this finding is limited due to the small sample size ($n = 48$) and

Table 2. Urinary 8-OHdG concentrations by serum ferritin levels

	Ferritin tertile (ng/mL)	Geometric mean (95% CI) of 8-OHdG concentrations (μg/g creatinine)						
		n	Unadjusted	Model 1†	*n*	Model 2‡	*n*	Model 3§
Women <50 years	<17	51	1.80 (1.61–2.00)	1.90 (1.65–2.20)	51	2.16 (1.82–2.56)	51	1.91 (1.63–2.24)
	17–35	51	2.93 (2.69–3.19)	3.04 (2.60–3.56)	51	3.20 (2.73–3.75)	51	3.00 (2.52–3.58)
	≥36	52	4.19 (3.82–4.61)	4.37 (3.76–5.08)	52	4.57 (3.92–5.33)	49	4.39 (3.71–5.19)
	P for trend		<0.001	<0.001		<0.001		<0.001
Women ≥50 years	<25	20	2.03 (1.69–2.43)	1.66 (1.16–2.37)	20	1.84 (1.22–2.76)	20	1.44 (1.01–2.04)
	25–84	20	3.57 (3.05–4.19)	2.87 (1.91–4.30)	20	3.11 (2.02–4.77)	20	2.24 (1.47–3.39)
	≥85	21	4.87 (4.21–5.64)	3.92 (2.49–6.16)	21	4.19 (2.64–6.64)	21	3.41 (2.21–5.28)
	P for trend		<0.001	<0.001		<0.001		<0.001
Men	<98	105	2.47 (2.30–2.65)	2.47 (2.32–2.63)	99	2.38 (2.21–2.56)	105	2.45 (2.30–2.61)
	98–179	102	3.22 (3.03–3.43)	3.17 (2.98–3.38)	97	3.05 (2.83–3.28)	98	3.24 (3.03–3.47)
	≥180	106	3.56 (3.36–3.77)	3.59 (3.35–3.83)	98	3.39 (3.13–3.68)	106	3.58 (3.34–3.84)
	P for trend		<0.001	<0.001		<0.001		<0.001

†Adjusted for age, smoking status, and body mass index. ‡Adjusted for age, smoking status, body mass index, and hemoglobin.
§Adjusted for age, smoking status, body mass index, alcohol consumption, physical activity, vitamin C and vitamin E intake. 8-OHdG, 8-hydroxydeoxyguanosine; CI, confidence interval.

doi: 10.1111/j.1349-7006.2009.01394.x

subjects' profile (dyslipidemic men), which may not represent the general population. In another study in a health checkup setting,[18] the correlation coefficient between serum ferritin and urinary 8-OHdG concentrations were 0.32 and 0.54 for men and women, respectively. However, the source population of the health checkup attendants was not clearly defined and no consideration was made for potentially important confounders including smoking. The observed association in our study (Spearman rank correlation coefficient, 0.47 and 0.76 for men and women, respectively) appears stronger than those documented previously. Our study participants shared a similar social background (municipal employees) and the survey was conducted in a short period of time (less than 10 days for each survey). We believe that such study design might have contributed to the minimization of the confounding effect of unmeasured variables.

Epidemiologic studies have reported an increased cancer risk associated with menopause[34] or high body iron status[35] in women. In the present study, women aged 50 years or older had markedly higher ferritin concentrations than did women aged less than 50 years, whereas hemoglobin levels did not differ. Although we did not obtain information regarding menopausal status from the study participants, given that the human body does not have a specific excretion route for stored iron[36], this probably reflected an increase of body iron storage after menopause. Moreover, in accordance with the difference of ferritin concentrations, women aged 50 or older had significantly higher 8-OHdG levels than women aged less than 50 years, suggesting an increased oxidative DNA damage after menopause. Because the regression line of serum ferritin concentrations on urinary 8-OHdG levels was similar between the two women's age groups, the increased levels of oxidative DNA damage among the older women could be ascribed to their elevated body iron storage, rather than to decreased physiologic function against oxidative stress after menopause.

Several epidemiologic studies have shown an increased risk of cancer associated with high dietary intake of heme iron[5,6] and high blood levels of iron.[7–10] Moreover, as a phlebotomy intervention study indicated,[11] iron reduction may decrease cancer risk even among persons without iron metabolism disorders. Together with accumulating data for the usefulness of urinary 8-OHdG as a marker of cancer risk,[15–17] the strong positive association between serum ferritin concentrations and urinary 8-OHdG concentrations in the present study supports the hypothesis that body iron storage increases cancer risk through oxidative DNA damage in humans.

Major strengths of the present study include high participation rate (91%), adjustment of potential confounding variables in the analysis, and use of a reliable method for 8-OHdG measurement (HPLC). Our study has also some limitations. First, causality can not be inferred from any cross-sectional study, like ours. Second, we measured biomarker levels only at a single point in time, which may not represent long-term status. Third, other biomarkers of body iron including transferrin saturation or soluble transferrin receptor[37] were not measured in the present study. However, ferritin is considered a preferred marker for the assessment of iron-related oxidative stress.[38] Finally, the study subjects were healthy municipal workers, and thus caution should be exercised when applying the result to populations with a different background.

In conclusion, we found a strong positive association between urinary 8-OHdG levels and serum ferritin concentrations in Japanese workers. This finding suggests that body iron storage is an important determinant of oxidative DNA damage, and thus supports a significant role for iron in carcinogenesis in a general population. The observed cross-sectional association requires confirmation in longitudinal studies.

Acknowledgments

This work was supported by a Grant-in-Aid for the Third Term Comprehensive 10-Year Strategy for Cancer Control from the Ministry of Health, Labour and Welfare of Japan; and Grant-in-Aids for Scientific Research (C) (no. 18590601) and (B) (no. 21390213) from the Japan Society for the Promotion of Science. We are grateful to Professor Hideki Igisu and Professor Hatsumi Taniguchi (University of Occupational and Environmental Health, Japan) for their guidance. We thank Tamani Hatano, Yasumi Kimura, Akihoro Takana, and Yoko Ejima (Kyushu University); Mio Ozawa (Fukuoka Women's University); and Akiko Hayashi and Kie Nagao (International Medical Center of Japan) for their help in data collection.

References

1 Halliwell B, Gutteridge JMC. *Free Radicals in Biology and Medicine*, 4th edn. New York: Oxford University Press, 2007; 220–36.
2 Valko M, Rhodes CJ, Moncol J, Izakovic M, Mazur M. Free radicals, metals and antioxidants in oxidative stress-induced cancer. *Chem Biol Interact* 2006; **160**: 1–40.
3 Toyokuni S. Iron-induced carcinogenesis: the role of redox regulation. *Free Radic Biol Med* 1996; **20**: 553–66.
4 Sawa T, Akaike T, Kida K, Fukushima Y, Takagi K, Maeda H. Lipid peroxyl radicals from oxidized oils and heme-iron: implication of a high-fat diet in colon carcinogenesis. *Cancer Epidemiol Biomarkers Prev* 1998; **7**: 1007–12.
5 Lee DH, Anderson KE, Folsom AR, Jacobs DR, Jr. Heme iron, zinc and upper digestive tract cancer: the Iowa Women's Health Study. *Int J Cancer* 2005; **117**: 643–7.
6 Zhou W, Park S, Liu G *et al.* Dietary iron, zinc, and calcium and the risk of lung cancer. *Epidemiology* 2005; **16**: 772–9.
7 Hann HW, Kim CY, London WT, Blumberg BS. Increased serum ferritin in chronic liver disease: a risk factor for primary hepatocellular carcinoma. *Int J Cancer* 1989; **43**: 376–9.
8 Knekt P, Reunanen A, Takkunen H, Aromaa A, Heliovaara M, Hakulinen T. Body iron stores and risk of cancer. *Int J Cancer* 1994; **56**: 379–82.
9 Selby JV, Friedman GD. Epidemiologic evidence of an association between body iron stores and risk of cancer. *Int J Cancer* 1988; **41**: 677–82.
10 Stevens RG, Graubard BI, Micozzi MS, Neriishi K, Blumberg BS. Moderate elevation of body iron level and increased risk of cancer occurrence and death. *Int J Cancer* 1994; **56**: 364–9.
11 Zacharski LR, Chow BK, Howes PS *et al.* Decreased cancer risk after iron reduction in patients with peripheral arterial disease: results from a randomized trial. *J Natl Cancer Inst* 2008; **100**: 996–1002.
12 Cross AJ, Gunter MJ, Wood RJ *et al.* Iron and colorectal cancer risk in the alpha-tocopherol, beta-carotene cancer prevention study. *Int J Cancer* 2006; **118**: 3147–52.
13 Kato I, Dnistrian AM, Schwartz M *et al.* Iron intake, body iron stores and colorectal cancer risk in women: a nested case-control study. *Int J Cancer* 1999; **80**: 693–8.
14 Zacharski LR, Chow BK, Howes PS *et al.* Reduction of iron stores and cardiovascular outcomes in patients with peripheral arterial disease: a randomized controlled trial. *JAMA* 2007; **297**: 603–10.
15 Loft S, Svoboda P, Kasai H *et al.* Prospective study of 8-oxo-7,8-dihydro-2′-deoxyguanosine excretion and the risk of lung cancer. *Carcinogenesis* 2006; **27**: 1245–50.
16 Cooke MS, Osborne JE, Singh R *et al.* Evidence that oxidative stress is a risk factor for the development of squamous cell carcinoma in renal transplant patients. *Free Radic Biol Med* 2007; **43**: 1328–34.
17 Thanan R, Murata M, Pinlaor S *et al.* Urinary 8-oxo-7,8-dihydro-2′-deoxyguanosine in patients with parasite infection and effect of antiparasitic drug in relation to cholangiocarcinogenesis. *Cancer Epidemiol Biomarkers Prev* 2008; **17**: 518–24.
18 Nakano M, Kawanishi Y, Kamohara S *et al.* Oxidative DNA damage (8-hydroxydeoxyguanosine) and body iron status: a study on 2507 healthy people. *Free Radic Biol Med* 2003; **35**: 826–32.
19 Kasai H, Iwamoto-Tanaka N, Miyamoto T *et al.* Life style and urinary 8-hydroxydeoxyguanosine, a marker of oxidative dna damage: effects of exercise, working conditions, meat intake, body mass index, and smoking. *Jpn J Cancer Res* 2001; **92**: 9–15.

20 Mizoue T, Tokunaga S, Kasai H, Kawai K, Sato M, Kubo T. Body mass index and oxidative DNA damage: a longitudinal study. *Cancer Sci* 2007; **98**: 1254–8.
21 Tuomainen TP, Loft S, Nyyssonen K, Punnonen K, Salonen JT, Poulsen HE. Body iron is a contributor to oxidative damage of DNA. *Free Radic Res* 2007; **41**: 324–8.
22 Kohgo Y, Ikuta K, Ohtake T, Torimoto Y, Kato J. Body iron metabolism and pathophysiology of iron overload. *Int J Hematol* 2008; **88**: 7–15.
23 Murakami K, Mizoue T, Sasaki S *et al.* Dietary intake of folate, other B vitamins, and omega-3 polyunsaturated fatty acids in relation to depressive symptoms in Japanese adults. *Nutrition* 2008; **24**: 140–7.
24 Kasai H, Svoboda P, Yamasaki S, Kawai K. Simultaneous determination of 8-hydroxydeoyguanosine, a marker of oxidative stress, and creatinine, a standardization compound, in urine. *Ind Health* 2005; **43**: 333–6.
25 Sasaki S. Development and evaluation of dietary assessment methods using biomarkers and diet history questionnaires for individuals. (Japanese) In: Tanaka H, ed. *Research for Evaluation Methods of Nutrition and Dietary Lifestyle Programs Held on Health Japan 21*. Summary report. Tokyo: Ministry of Health, Welfare, and Labour, 2004: 10–44.
26 Whitfield JB, Treloar S, Zhu G, Powell LW, Martin NG. Relative importance of female-specific and non-female-specific effects on variation in iron stores between women. *Br J Haematol* 2003; **120**: 860–6.
27 Amagai Y, Ishikawa S, Gotoh T, Kayaba K, Nakamura Y, Kajii E. Age at menopause and mortality in Japan: the Jichi Medical School Cohort Study. *J Epidemiol* 2006; **16**: 161–6.
28 Loft S, Vistisen K, Ewertz M, Tjonneland A, Overvad K, Poulsen HE. Oxidative DNA damage estimated by 8-hydroxydeoxyguanosine excretion in humans: influence of smoking, gender and body mass index. *Carcinogenesis* 1992; **13**: 2241–7.
29 Pilger A, Rudiger HW. 8-Hydroxy-2'-deoxyguanosine as a marker of oxidative DNA damage related to occupational and environmental exposures. *Int Arch Occup Environ Health* 2006; **80**: 1–15.
30 Cook JD, Lipschitz DA, Miles LE, Finch CA. Serum ferritin as a measure of iron stores in normal subjects. *Am J Clin Nutr* 1974; **27**: 681–7.
31 Torti FM, Torti SV. Regulation of ferritin genes and protein. *Blood* 2002; **99**: 3505–16.
32 Reif DW. Ferritin as a source of iron for oxidative damage. *Free Radic Biol Med* 1992; **12**: 417–27.
33 Carbonell T, Rama R. Iron, oxidative stress and early neurological deterioration in ischemic stroke. *Curr Med Chem* 2007; **14**: 857–74.
34 Van Asperen IA, Feskens EJ, Bowles CH, Kromhout D. Body iron stores and mortality due to cancer and ischaemic heart disease: a 17-year follow-up study of elderly men and women. *Int J Epidemiol* 1995; **24**: 665–70.
35 Hercberg S, Estaquio C, Czernichow S *et al.* Iron status and risk of cancers in the SU.VI.MAX cohort. *J Nutr* 2005; **135**: 2664–8.
36 Siah CW, Ombiga J, Adams LA, Trinder D, Olynyk JK. Normal iron metabolism and the pathophysiology of iron overload disorders. *Clin Biochem Rev* 2006; **27**: 5–16.
37 Cook JD, Flowers CH, Skikne BS. The quantitative assessment of body iron. *Blood* 2003; **101**: 3359–64.
38 Lee DH, Zacharski LR, Jacobs DR , Jr. Comparison of the serum ferritin and percentage of transferrin saturation as exposure markers of iron-driven oxidative stress-related disease outcomes. *Am Heart J* 2006; **151**: 1247.e1,1247.e7.

doi: 10.1111/j.1349-7006.2009.01394.x

Experimental and Molecular Pathology 88 (2010) 90–95

Contents lists available at ScienceDirect

Experimental and Molecular Pathology

journal homepage: www.elsevier.com/locate/yexmp

RhoB enhances migration and MMP1 expression of prostate cancer DU145

Misao Yoneda [a], Yoshifumi S. Hirokawa [b,*], Atsuyuki Ohashi [b], Katsunori Uchida [b], Daisuke Kami [c], Masatoshi Watanabe [c], Toyoharu Yokoi [a], Taizo Shiraishi [b], Shinya Wakusawa [a]

[a] Department of Medical Technology, Nagoya University School of Health Sciences, 1-1-20 Minami, Daiko, Higashi-ku, Nagoya City, Aichi, Japan
[b] Department of Pathologic Oncology, Institute of Molecular and Experimental Medicine, Faculty of Medicine, Mie University Graduate School of Medicine, 2-174 Edobashi, Tsu, Mie 514-8507, Japan
[c] Laboratory for Medical Engineering, Division of Materials Science and Chemical Engineering, Graduate School of Engineering, Yokohama National University, Japan

ARTICLE INFO

Article history:
Received 27 March 2009
and in revised form 15 September 2009
Available online 24 September 2009

Keywords:
RhoB
GSK-3
MMP1
Prostate cancer

ABSTRACT

Rho family protein regulates variety of cellular functions as cytoskeletal organization, cell proliferation and apoptosis. In the present study, we demonstrate that RhoB-overexpressed prostate cancer cells showed an enhanced cell motility and the administration of the GSK-3 inhibitors inhibited this increase in migration. Among the extracellular matrix and adhesion-related molecules, MMP1 RNA expression was increased in RhoB-overexpressed cells, administration of MMP inhibitor suppressed the collagen gel invasion in these cells. This is the first report evaluating RhoB function and the downstream signaling events in prostate cancer cell. Our results indicate that RhoB promotes cell motility and invasion in a metastatic prostate cancer cell.

Introduction

Rho GTPase, RhoA, RhoB and RhoC regulate the organization of the cytoskeleton and cell motility (Wheeler and Ridley 2004). Among the Rho family of proteins, particular attention has been focused on RhoA, Rac1 and Cdc 42 since these molecules play central roles in cell migration through the regulation and formation of actin stress fiber, filopodia and lamellipodia, respectively (Ridley and Hall, 1992; Ridley et al., 1992; Kozma et al., 1995). The relevance of the subcellular RhoB localization at the endosome (Adamson et al., 1992), an RhoB function, is proposed to regulate membrane trafficking such as EGF receptor (Wherlock et al., 2004) and Src (Sandilands et al., 2004). In addition to its GTPase status, RhoB function is also influenced by the C terminal prenylated modification of either farnesylation or geranylgeranylation in apoptotic response, mitosis, tumor growth and actin organization (Liu et al., 2000; Moasser et al., 1998; Chen et al., 2000; Allal et al. 2002). The RhoB protein is induced by a variety of stimuli in vitro, including UV irradiation, cytokines and growth factors (Prendergast 2001). In vitro cancer model, RhoB overexpression, inhibits migration and invasion. RhoB suppresses melanoma metastasis in mouse xenograft model (Jiang et al., 2004). On the contrary, fibroblasts from RhoB knockout mice migrate less than the wild-type counterpart (Liu et al., 2001).

Processing and or degrading varieties of substrates in extracellular milieu, the matrix metalloproteinases (MMPs) play central roles in tissue remodeling, promoting cancer invasion and metastasis (Sternlicht and Werb 2001). MMP1 is associated with a poor prognosis of colon cancer (Murray et al., 1996), involved in the invasive potential of lung cancer (Schütz et al., 2002). The genetic variants of MMP1, that lead to a high protein expression, are epidemiologically linked with ovarian cancer, metastatic melanoma and lung cancer (Sternlicht and Werb 2001; Sauter et al., 2008).

In preliminary experiments, when a prostate cancer cell line DU145 was treated with reagents that promoted DNA demethylation and chromatin acetylation, RhoB RNA expression was stimulated to about ninety times the level of the untreated cells. Treating the same reagents of another prostate cancer cell line LNCap, RhoB expression was enhanced only about two times. Here we generated DU145 cell lines stably expressing RhoB and examined the effect of RhoB on cellular motility and invasion.

Materials and methods

Cell lines and reagents

The human RhoB cDNA was PCR amplified from the Clone Collection (Open Biosystems, EHS1001-7571211) and subcloned into the pcDNA3-HA vector. After introduction of the vector with or without the insert into the prostate cancer DU145 cell line, G418-selected clones were isolated. Up-regulation of the RhoB RNA/protein in these cells was confirmed. The SCADS inhibitor kit was generously supplied from Screening Committee of Anticancer Drugs supported by a Grant-in-Aid for Scientific Research on Priority Area "Cancer" from The Ministry of Education, Culture, Sports, Science and Technology, Japan. Two GSK-3 inhibitors, GSK-3 inhibitor IX (CalbioChem, 361550) and Indirubin-3′-monoxime-5-sulphonic acid (CalbioChem, 402085), were added to the culture at a final concentration of 10 μM.

* Corresponding author. Fax: +81 59 231 5210.
E-mail address: ultray2k@clin.medic.mie-u.ac.jp (Y.S. Hirokawa).

0014-4800/$ – see front matter © 2009 Elsevier Inc. All rights reserved.
doi:10.1016/j.yexmp.2009.09.010

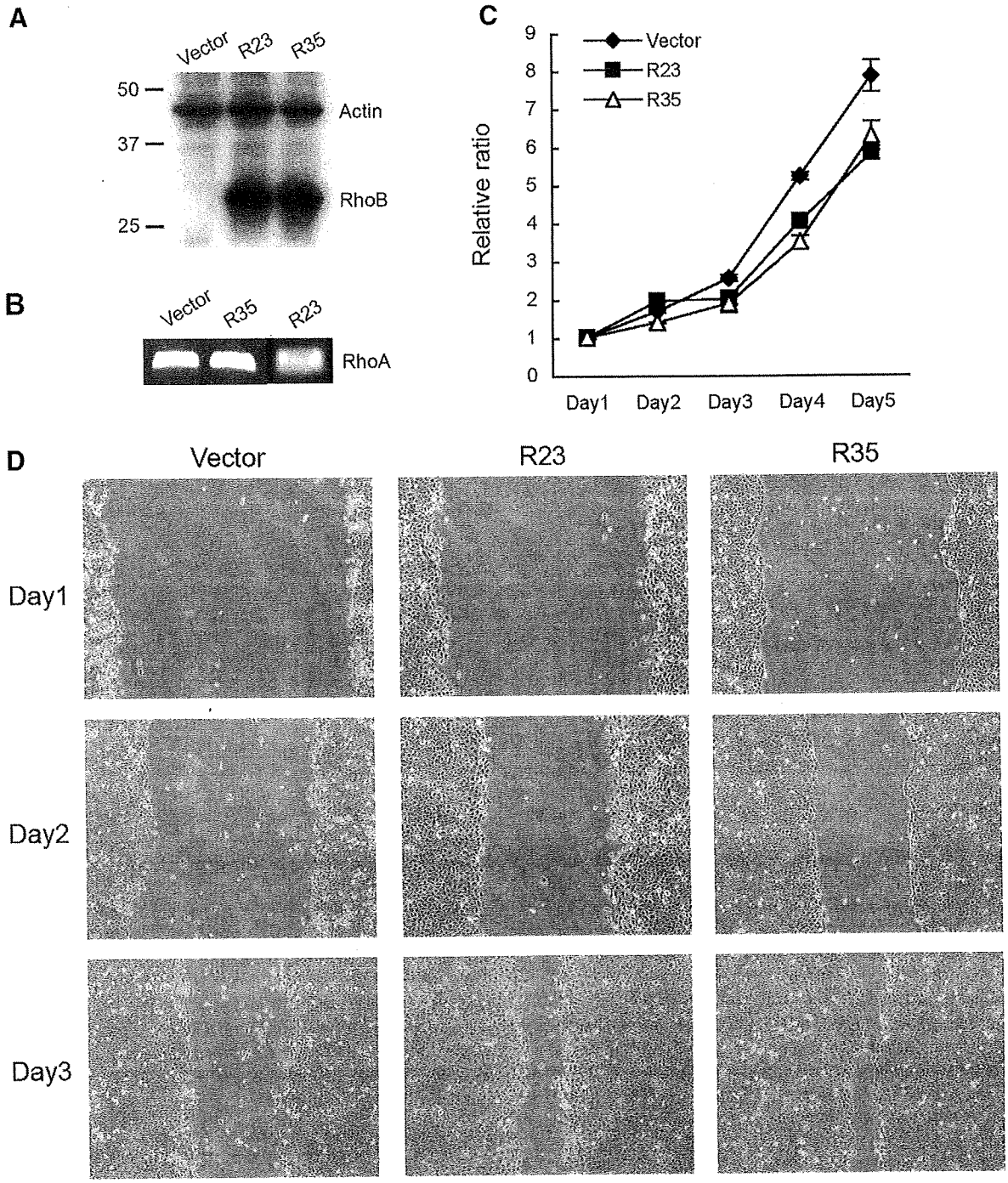

Fig. 1. RhoB overexpression promotes the migration of prostate cancer cells. (A) Western blot detection of two RhoB stably expressed clones R23 and R35 next to the vector-only-transfected clone. (B) RhoA mRNA expression levels in vector, R35 and R23 clone. (C) Cell growth up to 5 days culture are plotted as relative ratio to day 1. Data shown are mean ± SD of triplicates, representation from three independent experiments. (D) Wound closure assay with vector, R23 and R35 clones. Migration of each cell was observed for 3 days after the cells were scraped off. Images are representative of three independent experiments.

Wound closure/cell migration assays

The cells were cultured in RPMI 1640 (Sigma, R8758) with 10% fetal bovine serum (Gibco/Invitrogen) and seeded to a confluent density in 6 cm tissue culture dishes. For the wound closure assay, the monolayer of cells was scraped with the edge of a Cell Scraper (Iwaki, 9000-220). The cell migration assay was performed using the Boyden chamber method. Briefly, the cells were labeled with fluorescence Dil (Molecular Probes, D383) at 20 μg/ml in 6-cm tissue culture dishes for 6 h. Dil was dissolved in DMSO initially and then diluted in 100% EtOH. Dil-labeled 10^5 cells in 100-μl medium without FBS were loaded in the upper chamber (Falcon, 353097); the reagents from SCADS inhibitor kit and GSK-3 inhibitors were added to the bottom wells. After an overnight incubation, unmigrated cells were removed with a cotton swab, the chambers were placed in a new empty plate and the fluorescence of migrated cells was measured from the bottom direction using a plate reader.

The cell viability after administration of GSK-3 inhibitors was measured using the MTT assay according to the manufacturer's instructions (Promega, G3580). Each experiment was repeated at least twice in triplicate except for the SCADS inhibitor assay which was performed once because of the limited amount of the reagents.

Real-time PCR

Total RNA was isolated from prostate cancer cell lines using an RNA extraction kit according to the manufacturer's protocol (QIAGEN, 74104). First-strand cDNA synthesis was performed using the superscript II RNase Reverse Transcriptase kit (Invitrogen, 18080-044). The expression of 84 genes of the human extracellular matrix and adhesion molecules was analyzed according to the instructions of the RT^{2}Profiler PCR Array (SuperArray, PAHS-013A).

The primer sequences of RhoA were forward, 5′ TTACTCCGTAACA-GATTTTGTTGGC 3′, and reverse, 5′ ATACTACATCTAGTCTGGGGTAGAT 3′.

Collagen type I gel invasion assay

Invasion assays were carried out with a Cultrex 24-well collagen I cell invasion assay kit (3457-024-K) directed as the manufacture's instruction with a modification. Briefly, cells were cultured at 5×10^5 number in 6-cm plate, on the next day, 5×10^4 cells were suspended in 98 μl of RPMI 1640 with 0.5% fetal bovine serum, adding 2 μl of 5× collagen I solution, after mixing with pipeting, a 100-μl of cell/collagen mixed solution was aliquoted in each chamber (Falcon, 353097). Bottom well was loaded RPMI 1640 with 10% fetal bovine serum. After an overnight incubation, un-invaded cells were removed with a cotton swab, the chambers were placed back to the original wells with cell counting assay reagent (Cell Counting Kit-8, DOJINDO) and the absorbance of invaded cells was measured using a plate reader. Evaluating the MMP1 function of RhoB-overexpressed cells, MMP inhibitor II (CALBIOCHEM, #444247) was added to the medium of 6-cm plate at 100 μM and the cells were incubated for 6 h before the collagen gel chamber assay.

Both experiments were repeated three times in triplicate.

Results

RhoB overexpression enhanced prostate cancer cell migration

Two of the clones, designated R23 and R35, showed high RhoB protein expression compared to the vector-transfected clone (Fig. 1A). The proliferation rate at the culture conditions was slightly slower in R25 and R35 than vector-transfected cells, but this difference was not robust for the first three days (Fig. 1C). On culture days 4 and 5, vector-transfected cells grew faster than R25 and R35. Since RhoA also plays a pivotal role in cell proliferation, adhesion and migration, evaluating the RhoA status in prostate cancer cell migration under the test conditions was essential. The mRNA expression levels of RhoA were found to be similar in vector, R35 and R23 clone (Fig. 1B). When the migration rates were compared using the "wound closure assay", R23 and R35 showed faster movement than the vector clone in covering the "cellular defect" on the bottom of the scraped dish (Fig. 1D). This result clearly suggested the overexpression of the RhoB protein enhanced prostate cancer cell migration.

GSK-3 inhibitor suppressed migration of RhoB-expressed prostate cancer cells

In order to determine the signal mechanism underling the enhanced migration due to overexpression of the RhoB protein, an SCADS inhibitor kit was used for the migration assay. This kit includes several types of inhibitors commercially available. As described in the Materials and methods section, the initial cell migration was assessed by the Boyden chamber assay. Among the inhibitors inducing migratory suppression, GSK-3 inhibitors were chosen for the second round analysis. In cells treated with DMSO (vehicle), cell motility of R23 and R35 clones was twice that of the vector clone (Figs. 2A and B). Two of the GSK-3 inhibitors, GSK-3 inhibitor IX and Indirubin-3′-monoxime-5-sulphonic Acid, reduced the migration of R23 and R35 clones at the same level as that of the vector clone (Figs. 2A and B). Since the cell motility suppression was observed in the vector clone, GSK-3 inhibitors seemed to suppress endogenous RhoB effect as well. The cell viability of the three clones after treatment with GSK-3 inhibitors was not significantly different from each other (Fig. 2C).

Increased expression of MMP1 in RhoB-expressed prostate cancer and enhanced collagen gel invasion

Since cellular movement is closely associated with cell attachment, the mRNA levels of extracellular matrix and adhesion molecules were measured using real-time PCR (RT^{2}Profiler PCR Array). The most of gene expression levels were similar between R35 and vector clone (Table 1). The substantial fold changes between R35 versus vector clone were 2.36 of ADAM metallopeptidase with thrombospondin type 1 motif 8, 0.68 of E-cadherin, 0.55 of Vitronectin. Among the gene expression levels that were altered, MMP1 expression was about five times higher in the R35 clone than in the vector clone. The major substrates of MMP1 are collagens I, II and III. Verifying the functional relevance of MMP1 expression in the RhoB-overexpressed clones, chamber invasion assay was performed with type I collagen gel, which is the ubiquitously distributed interstitial matrix. Both R23 and R35 clones invaded through collagen gel more than vector clone (Fig. 3A). Prior to the chamber assay, incubating these cells with MMP inhibitor II, an inhibitor of MMP1, 3, 7 and 9, suppressed these enhanced cell invasion (Fig. 3B). These results indicate that MMP1 induction in RhoB-overexpressed prostate cancer cell is one of the mechanisms of increased migratory and invasive behavior of these cells.

Discussion

In the current study, we showed that the overexpression of RhoB enhanced cellular movement and invasion of prostate cancer cells in vitro. Increased motility is mediated by GSK-3 signaling and invasive potency is dependent on MMP1.

Previously, RhoB was shown to suppress the migration of NIH3T3 cells, invasion of pancreatic cancer cells and lung metastasis of melanoma cells (Jiang et al., 2004). RhoB-null macrophages also migrated faster on fibronectin (Wheeler and Ridley 2007). On the contrary, embryonic fibroblasts from an RhoB-null mouse showed less motility than wild-type fibroblasts in a wound closure test (Liu et al., 2001). Although the migratory mechanisms involved in these reverse functions of RhoB have not been fully elucidated yet, RhoB could play opposite roles within different cellular contexts. In NIH3T3 cells, GTPase-active and farnesylated RhoB can maintain an organized actin cytoskeleton and stress fibers against geranylgeranyl transferase inhibitor, which disrupts the actin cytoskeletal network (Allal et al., 2002). In this manner, the RhoB status of GTPase and prenylation could be different in each cellular type, consequently influencing actin fiber organization and cellular motility.

Fig. 2. GSK-3 inhibitors suppress motility of each cell clone in the chamber mobility assay. (A) Fluorescence microscope images of chamber membranes. Cells were plated inside the chamber in serum-free medium and allowed to migrate to serum and inhibitor-containing medium at the bottom for 12 h. (B) Migrated cell numbers were assessed in terms of the fluorescence value of each chamber. Data shown are mean ± SD of triplicates, representation from three independent experiments. (C) Cell viability of each clone was measured using the MTT assay after treatment of cells with GSK-3 inhibitors. Data shown are mean ± SD of triplicates, representation from two independent experiments.

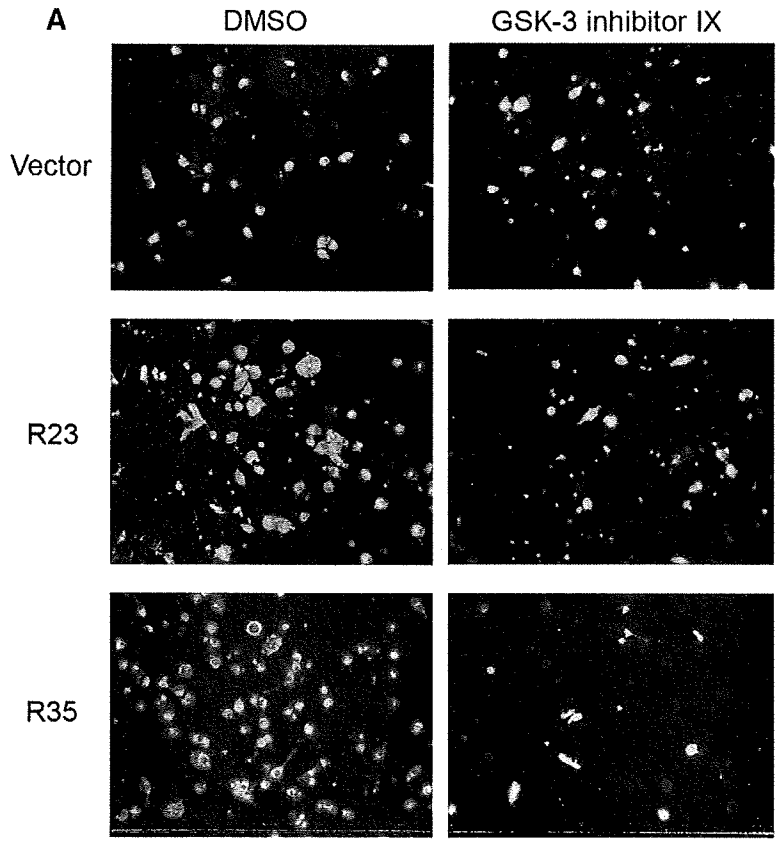
A
DMSO
GSK-3 inhibitor IX
Vector
R23
R35

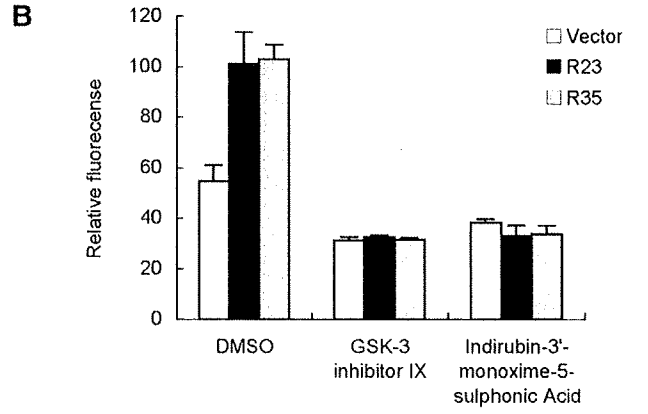
B
Relative fluorecense
120
100
80
60
40
20
0
Vector
R23
R35
DMSO
GSK-3 inhibitor IX
Indirubin-3'-monoxime-5-sulphonic Acid

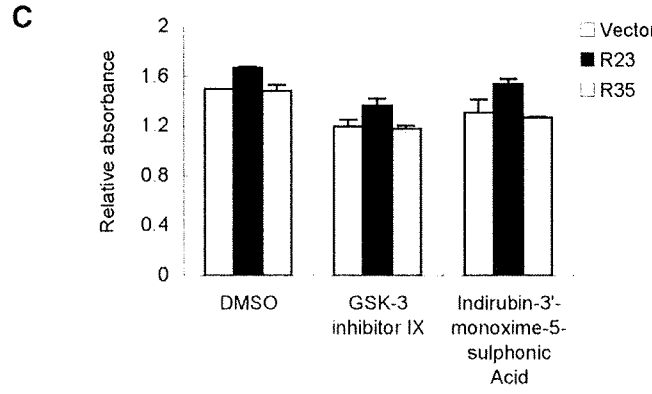
C
Relative absorbance
2
1.6
1.2
0.8
0.4
0
Vector
R23
R35
DMSO
GSK-3 inhibitor IX
Indirubin-3'-monoxime-5-sulphonic Acid

Table 1
Real-time PCR analysis of human extracellular matrix and adhesion molecules.

Gene	Fold change
ADAM metallopeptidase with thrombospondin type 1 motif, 1	1.03
ADAM metallopeptidase with thrombospondin type 1 motif, 13	0.96
ADAM metallopeptidase with thrombospondin type 1 motif, 8	2.36
CD44 molecule	1.18
Cadherin 1, E-cadherin	0.68
Contactin 1	0.84
Collagen, type XI, alpha 1	1.03
Collagen, type XII, alpha 1	0.39
Collagen, type XIV, alpha 1	1.03
Collagen, type XV, alpha 1	1.45
Collagen, type XVI, alpha 1	1.03
Collagen, type I, alpha 1	1.03
Collagen, type IV, alpha 2	1.92
Collagen, type V, alpha 1	1.03
Collagen, type VI, alpha 1	0.63
Collagen, type VI, alpha 2	0.73
Collagen, type VII, alpha 1	1.03
Collagen, type VIII, alpha 1	1.03
Versican	1.03
Connective tissue growth factor	0.63
Catenin, alpha 1	0.78
Catenin, beta 1	0.84
Catenin, delta 1	0.9
Catenin, delta 2	1.03
Extracellular matrix protein 1	1.67
Fibronectin 1	1.36
Hyaluronan synthase 1	1.03
Intercellular adhesion molecule 1 (CD54)	0.73
Integrin, alpha 1	1.18
Integrin, alpha 2 (CD49B)	1.56
Integrin, alpha 3 (antigen CD49C)	1.27
Integrin, alpha 4 (antigen CD49D)	1.03
Integrin, alpha 5 (fibronectin receptor)	0.73
Integrin, alpha 6	0.96
Integrin, alpha 7	1.03
Integrin, alpha 8	1.03
Integrin, alpha L (antigen CD11A)	1.03
Integrin, alpha M	1.03
Integrin, alpha V (vitronectin receptor)	1.1
Integrin, beta 1 (fibronectin receptor)	0.84
Integrin, beta 2	0.84
Integrin, beta 3 (antigen CD61)	1.03
Integrin, beta 4	1.67
Integrin, beta 5	1.03
Kallmann syndrome 1 sequence	1.03
Laminin, alpha 1	1.1
Laminin, alpha 2 (merosin)	1.03
Laminin, alpha 3	1.03
Laminin, beta 1	1.27
Laminin, beta 3	0.9
Laminin, gamma 1	0.78
Matrix metallopeptidase 1	5.06
Matrix metallopeptidase 10 (stromelysin 2)	1.03
Matrix metallopeptidase 11 (stromelysin 3)	0.78
Matrix metallopeptidase 12	1.03
Matrix metallopeptidase 13 (collagenase 3)	1.03
Matrix metallopeptidase 14	1.79
Matrix metallopeptidase 15	0.59
Matrix metallopeptidase 16	1.03
Matrix metallopeptidase 2	1.03
Matrix metallopeptidase 3 (stromelysin 1)	1.03
Matrix metallopeptidase 7 (matrilysin)	1.03
Matrix metallopeptidase 8	1.03
Matrix metallopeptidase 9	0.9
Neural cell adhesion molecule 1	1.03
Platelet/endothelial cell adhesion molecule (CD31 antigen)	1.03
Selectin E	1.03
Selectin L	0.84
Selectin P (antigen CD62)	1.03
Sarcoglycan, epsilon	0.84
Osteonectin	1.03
Spastic paraplegia 7	1.18
Secreted phosphoprotein 1 (osteopontin)	1.03
Transforming growth factor-beta	1.1
Thrombospondin 1	1.18
Thrombospondin 2	1.03
Thrombospondin 3	0.9
TIMP metallopeptidase inhibitor 1	1.67
TIMP metallopeptidase inhibitor 2	0.96
TIMP metallopeptidase inhibitor 3	1.03
C-type lectin domain family 3, member B	1.03
Tenascin C	1.79
Vascular cell adhesion molecule 1	1.03
Vitronectin	0.55
Beta-2-microglobulin	1.45
Hypoxanthine phosphoribosyltransferase 1	1.1

Fold changes of R35 to Vector clone were calculated according to the instructions of the RT^{2}Profiler PCR Array.

Because our data indicate that the GSK-3 inhibitors tested abrogated prostate cancer cell migration to the basal level, GSK-3 is postulated to play a pivotal role in cell motility under the RhoB-involved signal cascade. The role of RhoB in GSK-3 signaling has already been demonstrated under hypoxic conditions (Skuli et al., 2006). Hypoxic signals induced RhoB-dependent Akt and GSK-3 phosphorylation. An RhoB-overexpressed R35 cell line did not show predominantly phosphorylated Akt (Thr308 and Ser473, data not shown); thus, signal transduction to GSK-3 might bypass Akt activation in this cell line.

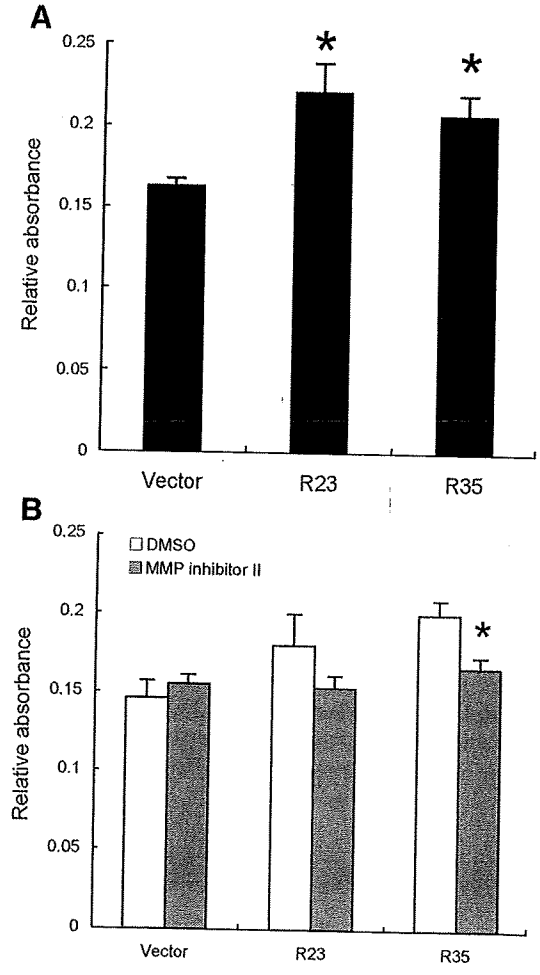

Fig. 3. Collagen gel invasion assays with or without MMP inhibitor. (A) Invasive potential of each clones were measured with Boyden chamber based assay system. Data shown are mean ± SD of triplicates, representation from three independent experiments. *$p<0.05$, compared to vector control. (B) Same collagen gel invasion assay in panel A, except each cells were pretreated with MMP inhibitor. Data shown are mean ± SD of triplicates, representation from three independent experiments. *$p<0.05$, compared to R35 DMSO. Mann–Whitney *U*-test was used to calculate statistical significances in panels A and B.

In addition to our current result, direct evidence showing that GSK-3 up-regulates epithelial cell migration has been presented using an MDCK wound closure assay (Farooqui et al., 2006). GSK-3 acts upstream of ADP-ribosylation factor 6 and Rac1, and the activated form of GSK-3 predominates during wound closure. The epithelial cell migration was blocked by an administration of GSK-3 inhibitor. The authors postulate that cell adhesion protein paxillin could be the downstream effecter molecule of GSK-3. Paxillin, which is a focal adhesion-associated protein, acts as a scaffold protein influencing cell motility and providing a signaling platform at the vicinity of focal adhesion (Brown and Turner, 2004). Since the phosphorylation of paxillin, which is essential in cell spreading, is mediated by GSK-3 and ERK dual-kinase (Cai et al., 2006), the phosphorylation levels of both proteins were evaluated in the R35 cell line. There was no difference in the phosphorylation status of GSK-3α (Ser21), GSK-3β (Ser9) and paxillin (Ser126) between R35 and vector cell lines (data not shown). GSK-3 phosphorylates target proteins preferably activated by other kinases (Doble and Woodgett, 2003). R35 and vector cells might have a different co-modifying set of kinases that target cell motile regulatory proteins.

Given the functional diversity, GSK-3 has been studied as a therapeutic target in many pathological conditions (Doble and Woodgett, 2003). Clinical and in vitro effects of GSK-3 inhibitors are insulin mimetic action, anti-cell proliferation and inhibition of tau phosphorylation. Recent studies have shown that administration of a GSK-3 inhibitor increased bone formation (Kulkarni et al., 2007) and prevented epithelial–mesenchymal transition (EMT) of human embryonic stem cell (Ullmann et al., 2008). EMT is the process of cytoskeletal and adhesion molecules to remodel an epithelial into mesenchymal phenotype, losing an original polarity but gaining a higher motility. Thus, close association of EMT with cancer invasion and metastasis, targeting GSK-3 by specific inhibitor, like our study and others, could become a therapeutic options for an advanced cancer.

The underlying mechanism between RhoB and MMP1 expression has not yet been fully elucidated. The cytoplasmic tail of a transmembrane mucin, MUC1, translocates to the nucleus after phosphorylation by Met, interacts with p53 and leads to the suppression of MMP1 transcription (Singh et al., 2008). MUC1 is also phosphorylated by GSK-3β (Li et al., 1998). The phosphorylation sites of MUC1 by Met and GSK-3β are not identical. So it is plausible that MUC1 in RhoB-overexpressed prostate cancer cells might be predominantly phosphorylated by GSK-3β, abrogating its suppressive effect on MMP1 transcription.

In the literature, there have been no solid data studying the relevance of RhoB and clinical cancer. One can assume that no correlation has been observed between clinical cancer and RhoB expression level. We did the compared real-time PCR experiment of RhoB in the cancer versus non-cancerous tissue from clinically dissected prostate cancer. The RhoB expression ratio (cancer/non-cancer) was diverse among each cancer cases and no correlation was observed toward Gleason score, an indicator of malignant potency and prognosis (data not shown). Based on the origin of DU145 cell line, which was derived from brain metastasis lesion, RhoB function as an invasion promoter might be exerted at distant metastatic prostate cancer. Even in this scenario, DNA demethylated and/or chromatin acetylated modification could be required for an induction of RhoB protein in prostate cancer cells as in our preliminary experiment.

In conclusion, this study presents the first evidence that RhoB promotes cellular motility and invasion of prostate cancer cell, signaling downstream in GSK-3 and enhancing a collagen gel invasion by MMP1 induction. Current results indicate that in certain cell type, like prostate cancer, RhoB works as a tumor promoter not as a suppressor. Unraveling the cell-type-specific bifunctional mechanisms and conditions of RhoB protein should help understanding the biological, physiological and pathological protein behavior.

References

Adamson, P., Paterson, H.F., Hall, A., 1992. Intracellular localization of the P21rho proteins. J. Cell Biol. 119, 617–627.

Allal, C., Pradines, A., Hamilton, A.D., Sebti, S.M., Favre, G., 2002. Farnesylated RhoB prevents cell cycle arrest and actin cytoskeleton disruption caused by the geranylgeranyltransferase I inhibitor GGTI-298. Cell Cycle 1, 430–437.

Brown, M.C., Turner, C.E., 2004. Paxillin adapting to change. Physiol. Rev. 84, 1315–1339.

Cai, X., Li, M., Vrana, J., Schaller, M.D., 2006. Glycogen synthase kinase 3- and extracellular signal-regulated kinase-dependent phosphorylation of paxillin regulates cytoskeletal rearrangement. Mol. Cell Biol. 26, 2857–2868.

Chen, Z., Sun, J., Pradines, A., Favre, G., Adnane, J., Sebti, S.M., 2000. Both farnesylated and geranylgeranylated RhoB inhibit malignant transformation and suppress human tumor growth in nude mice. J. Biol. Chem. 275, 17974–17978.

Doble, B.W., Woodgett, J.R., 2003. GSK-3: tricks of the trade for a multi-tasking kinase. J. Cell Sci. 116 (Part 7), 1175–1186.

Farooqui, R., Zhu, S., Fenteany, G., 2006. Glycogen synthase kinase-3 acts upstream of ADP-ribosylation factor 6 and Rac1 to regulate epithelial cell migration. Exp. Cell Res. 312, 1514–1525.

Jiang, K., Sun, J., Cheng, J., Djeu, J.Y., Wei, S., Sebti, S., 2004. Akt mediates Ras downregulation of RhoB, a suppressor of transformation, invasion, and metastasis. Mol. Cell. Biol. 24, 5565–5576.

Kozma, R., Ahmed, S., Best, A., Lim, L., 1995. The Ras-related protein Cdc42Hs and bradykinin promote formation of peripheral actin microspikes and filopodia in Swiss 3T3 fibroblasts. Mol. Cell. Biol. 15, 1942–1952.

Kulkarni, N.H., Wei, T., Kumar, A., Dow, E.R., Stewart, T.R., Shou, J., N'cho, M., Sterchi, D.L., Gitter, B.D., Higgs, R.E., Halladay, D.L., Engler, T.A., Martin, T.J., Bryant, H.U., Ma, Y.L., Onyia, J.E., 2007. Changes in osteoblast, chondrocyte, and adipocyte lineages mediate the bone anabolic actions of PTH and small molecule GSK-3 inhibitor. J. Cell Biochem. 102, 1504–1518.

Li, Y., Bharti, A., Chen, D., Gong, J., Kufe, D., 1998. Interaction of glycogen synthase kinase 3beta with the DF3/MUC1 carcinoma-associated antigen and beta-catenin. Mol. Cell. Biol. 18, 7216–7224.

Liu, A., Du, W., Liu, J.P., Jessell, T.M., Prendergast, G.C., 2000. RhoB alteration is necessary for apoptotic and antineoplastic responses to farnesyltransferase inhibitors. Mol. Cell. Biol. 20, 6105–6113.

Liu, A.X., Rane, N., Liu, J.P., Prendergast, G.C., 2001. RhoB is dispensable for mouse development but it modifies susceptibility to tumor formation as well as cell adhesion and growth factor signaling in transformed cells. Mol. Cell. Biol. 20, 6906–6912.

Moasser, M.M., Sepp-Lorenzino, L., Kohl, N.E., Oliff, A., Balog, A., Su, D.S., Danishefsky, S.J., Rosen, N., 1998. Farnesyl transferase inhibitors cause enhanced mitotic sensitivity to taxol and epothilones. Proc. Natl. Acad. Sci. U. S. A. 95, 1369–1374.

Murray, G.I., Duncan, M.E., O'Neil, P., Melvin, W.T., Fothergill, J.E., 1996. Matrix metalloproteinase-1 is associated with poor prognosis in colorectal cancer. Nat. Med. 2, 461–462.

Prendergast, G.C., 2001. Actin' up RhoB in cancer and apoptosis. Nat. Rev. Cancer 1, 162–168.

Ridley, A.J., Hall, A., 1992. The small GTP-binding protein rho regulates the assembly of focal adhesions and actin stress fibers in response to growth factors. Cell 70, 389–399.

Ridley, A.J., Paterson, H.F., Johnston, C.L., Diekmann, D., Hall, A., 1992. The small GTP-binding protein rac regulates growth factor-induced membrane ruffling. Cell 70, 401–410.

Sandilands, E., Cans, C., Fincham, V.J., Brunton, V.G., Mellor, H., Prendergast, G.C., Norman, J.C., Superti-Furga, G., Frame, M.C., 2004. RhoB and actin polymerization coordinate Src activation with endosome-mediated delivery to the membrane. Dev. Cell 7, 855–869.

Sauter, W., Rosenberger, A., Beckmann, L., Kropp, S., Mittelstrass, K., Timofeeva, M., Wölke, G., Steinwachs, A., Scheiner, D., Meese, E., Sybrecht, G., Kronenberg, F., Dienemann, H., Chang-Claude, J, Illig, T., Wichmann, H.E., Bickeböller, H., Risch, A., LUCY-Consortium, 2008. Matrix metalloproteinase 1 (MMP1) is associated with early-onset lung cancer. Cancer Epidemiol. Biomarkers Prev. 17, 1127–1135.

Schütz, A., Schneidenbach, D., Aust, G., Tannapfel, A., Steinert, M., Wittekind, C., 2002. Differential expression and activity status of MMP-1, MMP-2 and MMP-9 in tumor and stromal cells of squamous cell carcinomas of the lung,. Tumour. Biol. 23, 179–184.

Singh, P.K., Behrens, M.E., Eggers, J.P., Cerny, R.L., Bailey, J.M., Shanmugam, K., Gendler, S.J., Bennett, E.P., Hollingsworth, M.A., 2008. Phosphorylation of MUC1 by Met modulates interaction with p53 and MMP1 expression. J. Biol. Chem. 283, 26985–26995.

Skuli, N., Monferran, S., Delmas, C., Lajoie-Mazenc, I., Favre, G., Toulas, C., Cohen-Jonathan-Moyal, E., 2006. Activation of RhoB by hypoxia controls hypoxia-inducible factor-1alpha stabilization through glycogen synthase kinase-3 in U87 glioblastoma cells. Cancer Res. 66, 482–489.

Sternlicht, M.D., Werb, Z., 2001. How matrix metalloproteinases regulate cell behavior. Annu. Rev. Cell Dev. Biol. 17, 463–516.

Ullmann, U., Gilles, C., De Rycke, M., Van de Velde, H., Sermon, K., Liebaers, I., 2008. GSK-3-specific inhibitor-supplemented hESC medium prevents the epithelial–mesenchymal transition process and the up-regulation of matrix metalloproteinases in hESCs cultured in feeder-free conditions. Mol. Hum. Reprod. 14, 169–179.

Wheeler, A.P., Ridley, A.J., 2004. Why three Rho proteins? RhoA, RhoB, RhoC, and cell motility. Exp. Cell Res. 301, 43–49.

Wheeler, A.P., Ridley, A.J., 2007. RhoB affects macrophage adhesion, integrin expression and migration. Exp. Cell Res. 313, 3505–3516.

Wherlock, M., Gampel, A., Futter, C., Mellor, H., 2004. Farnesyltransferase inhibitors disrupt EGF receptor traffic through modulation of the RhoB GTPase. J. Cell Sci. 117 (Part 15), 3221–3231.